Behavioural Brain Research 362 (2019) 7–20

Contents lists available at ScienceDirect

Behavioural Brain Research

journal homepage: www.elsevier.com/locate/bbr

Research report

Adeno-associated viral overexpression of neuroligin 2 in the mouse hippocampus enhances GABAergic synapses and impairs hippocampal-dependent behaviors

M. Van Zandt, E. Weiss, A. Almyasheva, S. Lipior, S. Maisel, J.R. Naegele*

Wesleyan University, Department of Biology, Program in Neuroscience and Behavior, Middletown, CT, United States

GRAPHICAL ABSTRACT

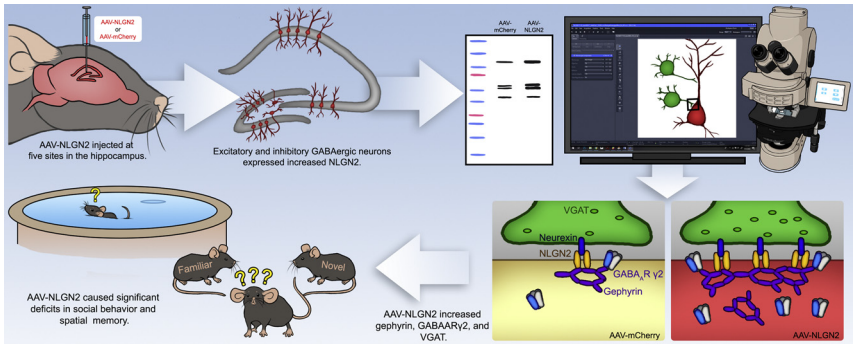

ARTICLE INFO

Keywords:
Neuroligin
Gephyrin
VGAT
Sociability
Social dominance
Spatial memory

ABSTRACT

The cell adhesion molecule neuroligin2 (NLGN2) regulates GABAergic synapse development, but its role in neural circuit function in the adult hippocampus is unclear. We investigated GABAergic synapses and hippocampus-dependent behaviors following viral-vector-mediated overexpression of NLGN2. Transducing hippocampal neurons with AAV-NLGN2 increased neuronal expression of NLGN2 and membrane localization of GABAergic postsynaptic proteins gephyrin and $GABA_AR\gamma2$, and presynaptic vesicular GABA transporter protein (VGAT) suggesting trans-synaptic enhancement of GABAergic synapses. In contrast, glutamatergic postsynaptic density protein-95 (PSD-95) and presynaptic vesicular glutamate transporter (VGLUT) protein were unaltered. Moreover, AAV-NLGN2 significantly increased parvalbumin immunoreactive (PV^+) synaptic boutons co-localized with postsynaptic $gephyrin^+$ puncta. Furthermore, these changes were demonstrated to lead to cognitive impairments as shown in a battery of hippocampal-dependent mnemonic tasks and social behaviors.

1. Introduction

Of the neuroligin (NLGN) family of synaptic proteins (NLGN1-4) only NLGN2 is selectively found at inhibitory synapses [1–4]. The NLGN proteins are integral membrane adhesion molecules that bind to presynaptic neurexins [5–8]. As mutations in NLGNs have been

Abbreviations: CA3, cornu ammonis 3; CA1, cornu ammonis 1; NLGN2, neuroligin2; GABA, gamma-aminobutyric acid; VGAT, vesicular GABA transporter; GCL, granule cell layer; MOL, molecular layer; DG, dentate gyrus; AAV, adeno-associated virus; SDS-PAGE, sodium dodecyl sulfate-polyacrylamide gel electrophoresis

* Corresponding author.
E-mail address: jnaegele@wesleyan.edu (J.R. Naegele).

https://doi.org/10.1016/j.bbr.2018.12.052
Received 2 August 2018; Received in revised form 14 December 2018; Accepted 29 December 2018
Available online 31 December 2018
0166-4328/

identified in patients with autism [9–11], schizophrenia [12], and other neurological disorders [13,14], the role of NLGN2 in inhibitory synapse formation, maturation, and function is of considerable interest. The expression of NLGN2 in vitro in non-neuronal cells induces putative synaptic contacts [8,15–17] and in vivo, binding between presynaptic neurexin and postsynaptic NLGN2 enhances inhibitory synaptic transmission [18]. NLGN2 tethers GABA receptors within a scaffold on the postsynaptic neuron through molecular interactions with gephyrin and collybistin [3]. By recruiting gephyrin and $GABA_A$Rs, NLGN2 shapes mature electrophysiological response properties [19,20].

Several studies have utilized genetic deletion or viral-vector-mediated overexpression to test whether dysregulation of NLGN2 causes GABAergic circuit dysfunction or cognitive changes with conflicting results. While genetically-induced NLGN2 deficiency or overexpression increase anxiety-like behaviors [21–24], limiting NLGN2 overexpression to the adult mouse dorsal hippocampus did not alter anxiety phenotypes [25]. Furthermore, regardless of whether NLGN2 expression was experimentally increased or decreased, preference ratios in the three-chamber sociability test were abolished [22,26,27]. Others found that constitutive NLGN2 knockout in the whole brain [23] or selective overexpression of NLGN2 in the adult rat hippocampus [25] did not alter social behavior. Aggression, as measured by the resident intruder test, also showed variable results between overexpression studies [25,27].

As a step toward addressing gaps in our understanding of the role of NLGN2 in inhibitory synapse formation and function in the adult brain, we increased NLGN2 expression in the DG and hippocampal subfields CA3 and CA1 in normal, naïve mice through adeno-associated viral (AAV) vectors and studied recruitment of synapse-specific presynaptic and postsynaptic molecules using immunohistochemistry, confocal microscopy, and biochemistry. Given the distinct functional roles for GABAergic cell types in the DG and CA subfields of the hippocampus [28] and the significant roles of GABAergic connections with hippocampal principle cells in regulating social behaviors [29,30], spatial memory [31,32], and brain rhythms [33–38], we also investigated whether NLGN2 overexpression altered social dominance, social memory, spatial memory, novel object recognition, object location, and anxiety.

2. Materials and methods

2.1. Experimental animals

All animal use followed protocols approved by the Wesleyan University's Institutional Animal Care and Use Committee. Male wild-type C57BL/6NHsd mice (Envigo; 8–10 weeks old, approximately 24–30 g) and VGAT-ChR2-eYFP mice (Jackson; 8–10 weeks old, approximately 24–30 g) were pair-housed in our animal facility in self-ventilating cage units, maintained on a 12-hour light/dark cycle, and provided with food and water ad libitum. A total of 51 mice were used for this study; 29 received stereotaxic injections into the hippocampus of the AAV-NLGN2 vector and 22 received stereotaxic injections of the control vector, AAV-mCherry. C57BL/6NHsd adult males were used for all behavioral and biochemistry experiments and both C57BL/6NHsd and VGAT-ChR2-eYFP adult male mice [39] were used for immunohistochemical studies. Behavioral testing was performed on 44 adult male C57BL/6NHsd mice; 24 received AAV-NLGN2 and 20 received AAV-mCherry injections. Prior to behavioral testing, mice were pair-housed with like-treated littermates and received handling for a week.

2.2. Viral constructs for overexpression of NLGN2

AAV/DJ mixed serotype viruses with CMV promoter-driven gene expression were used (Vector Biolabs). The NLGN2 vector contained the mouse NLGN2 gene (NM_198862) and an mCherry fluorescent reporter. The resulting custom plasmid (pAAV-cDNA6-mCherry-NLGN2) was packaged into AAV/DJ (Addgene; AAV/DJ-cDNA6-mCherry-NLGN2; titer: 1.3×10^{13} GC/mL). The control vector contained the CMV promoter driving expression of mCherry minus NLGN2 (AAV/DJ-CMV-mCherry; titer: 1.8×10^{13} GC/ml). Both vectors resulted in strong transduction of hippocampal neurons and robust expression for at least 4–6 weeks, the longest period that we tested.

2.3. Stereotaxic surgery

Mice were initially injected with Medicam (0.03 mL, s.c., Henry Schein) and stereotaxic injections of virus were made under isoflurane gas anesthesia (VetEquip, Harvard Apparatus). Each mouse received 0.5 µl of AAV vector/site (0.2 µl/minute) into 5 sites per hippocampus by means of an automated stereotaxic injection system (Stoelting Quintessential), equipped with a 5 µl glass syringe (Hamilton 7633-01) and bevel-tip needle (Hamilton, 30°, 30 gauge, 0.5"). The coordinates for anterior hippocampal injections were determined as follows: AP (Bregma – Lambda)/2; ML +/−1.25 mm; DV 2.2, 2.0, and 1.3 mm [40]. The coordinates for posterior injections were determined as follows: AP −3.0 – −.9 – (Bregma – Lambda)/2), ML ± 3.5, DV −4.0 and −3.0.

2.4. Behavioral assays

We conducted behavioral analyses 2–3 weeks post-AAV injections, then euthanized the mice for either biochemistry or immunohistochemistry. Each mouse was acclimated in its home cage in the behavioral testing facility 30 min prior to behavioral testing and apparatuses were wiped down with 75% ethanol between tests. The order of behavioral testing was: Open Field, Zero Maze, Novel Object Location, Novel Object Recognition, Sociability test, Social Dominance test, and the Morris Water Maze (Table S1). Testing was conducted under 16–22 lx illumination with ambient white noise while video recording, and later analyzed with AnyMaze software by a trained-observer blind to the treatment group.

Open Field testing to evaluate exploration and anxiety was performed in a white plastic circular arena, elevated approximately 86 cm from the ground, with 46 cm high sides and 91.4 cm inner diameter. The mouse was placed in the center of the arena and allowed to explore for 10 min. The distance traveled and time in the central area (designated by a circle of approximately 60 cm) were measured.

We also measured anxiety behavior with the Zero maze. As described previously, performance in this maze is relatively stable over time, as compared to the elevated plus maze [41]. The Zero maze consisted of an elevated circular platform with two open and two enclosed zones (inside diameter 61 cm; outside diameter 86.4 cm; platform elevation above the floor 77.5 cm; wall height 8.1 cm; camera height 223.5 cm). To initiate testing, the mice were placed facing an enclosed zone then allowed to explore the apparatus for 5 min. Mice the fell off the open arms of the apparatus were placed back on the maze and retested. The total distance travelled and time spent in each zone were quantified.

To test to test spatial memory, we used to two behavioral tests; the novel object recognition test and the object new location test. Both were performed in a square plastic arena (30.5 cm^2). Each mouse was acclimated to the arena for 10 min the day prior to testing. For novel object recognition, the mice were allowed to investigate 2 objects placed into opposite corners of the arena for 10 min. Objects included: 50 mL conical tubes filled with marbles, three 15 mL conical tubes taped together, and 100 mL plastic bottles with varying labels, all weighted to prevent displacement. One hour following the initial exposure, one of the objects was replaced with a different object of similar size, and the mice were allowed to investigate the objects for 10 min. For the object new location test, two objects were placed into opposite corners of the apparatus and the mice were allowed to investigate for

10 min. One hour later, one of the objects was relocated and the mice were allowed to investigate for 10 min. An area extending 1 inch in all directions around each object was designated as the area of interaction. The number of entries and the duration of time that the mouse's head was within this area were computed.

Social interactions were measured with Crawley's three-chambered sociability test in clear Plexiglass apparatus with three 20 cm by 40.5 cm interconnected chambers. Circular cages were placed in the two outer chambers (diameter 10 cm) and testing was conducted as previously described [42–44]. The mouse to be tested was placed in the central chamber with the doors shut and allowed to acclimate for 1 min. For the first round of testing, one cage contained a stranger mouse and the other was empty. The doors were then opened, and the mouse explored the apparatus freely for 10 min. The mouse was moved back into the central chamber and the doors were shut. A novel stranger mouse was placed in the previously empty cage and the experimental mouse was again allowed to explore the apparatus for 10 min. Interaction times and number of interactions were quantified. The area of interaction was designated as the area containing the social interaction cage area with a 3-cm border. The number of entries and the duration of time that the mouse's head was within this area were computed.

The social dominance apparatus consisted of an elevated clear Plexiglas tube (3 cm above table) [45]. Pairs of mice were placed in the opposite ends of the tube and allowed to meet in the center. The first mouse backing out of the tube was considered the "loser" of the bout, while the mouse remaining in the tube was considered the "winner". Testing lasted until one mouse backed out of the tube, or until 3 min elapsed; if neither mouse backed out, it was considered a draw. Bouts within experimental group were used to confirm that the mice exhibited normal dominance behavior and then we quantified bouts between the AAV-NLGN2 vs. AAV-mCherry groups of mice. Any mice showing < 0.2 or > 0.8 ratios within experimental group were excluded (2 AAV-mCherry mice, 0 AAV-NLGN2 mice).

Spatial memory was tested in a circular Morris Water Maze pool (122 cm diameter, 76 cm depth) filled with water (20 °C) made opaque with non-toxic white paint and enclosed by white curtains with visual cues. Training to find a submerged platform (diameter 16 cm) was for five days, followed by a probe trial on the sixth day. Training consisted of four training trials/day/mouse, lasting 60 s/trial, or until the mouse climbed on the platform. The mice remained on the platform for 10 s; if they failed to reach the platform, they were guided there. During the first two days of training only, a visual cue was placed on the platform. During the 60-sec probe trial on the sixth day, the platform was removed, and the swim speed, escape latency to the platform during training, latency to first platform area crossing in the probe trial, the number of platform area crossings in the probe trail, and the quadrant dwell time were measured.

2.5. Western blot analyses of adult mouse hippocampi

To harvest hippocampal tissue, the mice were euthanized using cervical dislocation and the left and right hippocampi were extracted and frozen at −80 °C. Membrane fractions were prepared by thawing the tissue in 400 µl of ice-cold TEVP buffer (10 mM Tris, pH 7.4, 5 mM NaF, 1 mM EDTA, and 1.0 mM EGTA, 1 mM Na_3VO_4) containing 320 mM sucrose with protease inhibitor and homogenizing with a dounce homogenizer. Samples were centrifuged for 10 min at 2500 rpm (Eppendorf 5415 C), the supernatant was extracted, and centrifuged for 15 min at 10,000 rpm to obtain the P2 pellet. The P2 fraction was suspended in TEVP buffer and solubilized by 10 freeze-thaw cycles, then frozen in aliquots and stored at −80 °C. Protein concentrations were calculated with a BCA assay kit (Thermo Scientific 23227).

SDS-PAGE was performed with a mini-gel electrophoresis system (Bio-Rad 525BR) with 4–20% precast gradient gels (Bio-Rad 4561091S). The membrane fractions from control and experimental mice run together on the same gels for comparison (20 µg protein/lane) and proteins were separated at a constant voltage (150 V) for 120 min and transferred onto PVDF membranes (Bio-Rad 153BR) with constant voltage (100 V) for 90 min. The transferred proteins were visualized by staining the PVDF membranes in Ponceau S, then the blots were cut into horizontal strips at 150, 75, 50 and 37 kDa, based on the migration of protein standards (Precision Plus Protein™ Dual Color Standards, BioRad #161-0374), to allow each lane to be probed with antibodies (see Table S1). The following antibodies were used: mouse anti-actin (1:2000), mouse anti-gephyrin (1:2000), rabbit anti-NLGN2 (1:4000), mouse anti-$GABA_AR\gamma2$ (1:4000), mouse anti-NR2B (1:1000), mouse anti-PSD95 (1:4000), and mouse anti-VGAT (1:8000). After washing the blots, the bound antibodies were detected by incubating in HRP-conjugated goat anti-mouse IgG (1:5000) or HRP-conjugated anti-rabbit IgG (1:10,000) followed by a 1-minute incubation in SuperSignal West Femto Maximum Sensitivity Substrate (ThermoFisher Scientific 34,096). The blots were imaged with GeneSnap software (SynGene 7.12) in a G:Box apparatus (Syngene G:Box Chemi XX6). Blot images were viewed in Image *J* software, inverted, and optical densities for each protein band were calculated. All values were normalized to actin within the same lane. Statistical analyses were performed using Student's *t*-test function, using each lane as a separate input.

2.6. Immunohistochemistry

For histology, the mice were euthanized (sodium pentobarbital, Henry Schein, 100 mg/kg, i.p.), and perfused transcardially (4% paraformaldehyde in 0.1 M phosphate buffer, pH 7.4). Cryostat sections were cut at 12 µm, mounted and immunostained on Superfrost Plus glass slides. Incubations were overnight at room temperature in primary antibodies diluted in 0.1 M sodium phosphate buffered saline containing 10% normal goat serum and 1% Triton-X 100. The following primary antibodies were used (see Table S1): chicken anti-GFP (1:1000), mouse anti-mCherry (1:1000), rabbit anti-mCherry (1:1000), chicken anti-mCherry (1:1000), rabbit anti-NLGN2 (1:1000), rabbit anti-parvalbumin (1:1000), guinea pig anti-VGAT (1:500), mouse anti-vGlut (1:500), and mouse anti-gephyrin (1:1000). Detection was performed with secondary antibodies (Life Technologies) and sections were mounted in Prolong Diamond with DAPI (Life Technologies).

2.7. Synaptic protein density analyses

Immunofluorescently labeled synaptic puncta were imaged by confocal microscopy at an optical slice interval of 0.33 µm (Zeiss LSM 510 Meta confocal microscope, C-Apochromat 63x objective 1.2 N.A.). The confocal images were analyzed in ImageJ with Puncta Analyzer [46]. We selected regions of interest (ROI) containing $mCherry^+$ neurons and then quantified co-localized synaptic protein labeling. Values were normalized based on mCherry expression within the ROI.

2.8. Quantification of putative synapses onto individual neurons

We quantified sites of putative synapses on granule and pyramidal cell somas by identifying puncta immunolabeled for presynaptic proteins (e.g. VGAT) that were in alignment with clusters of immunolabeled postsynaptic proteins (e.g. gephyrin). To ensure unbiased selection of AAV-labeled neurons, the images were viewed in the red channel and individual somas outlined, then the red channel was hidden, and the green and infrared channels were visualized. To quantify the number of putative synapses, we identified sites with alignment between immunolabeled presynaptic and postsynaptic proteins, and used Zeiss Zen software to generate a fluorescence histograms for these puncta. We set the background level based on the fluorescent intensity of an adjacent region without immunofluorescent staining in the same channel. Putative fluorescently labeled synaptic puncta were identified as peaks of fluorescently labeled pre- and postsynaptic markers that were both above background and in close proximity and

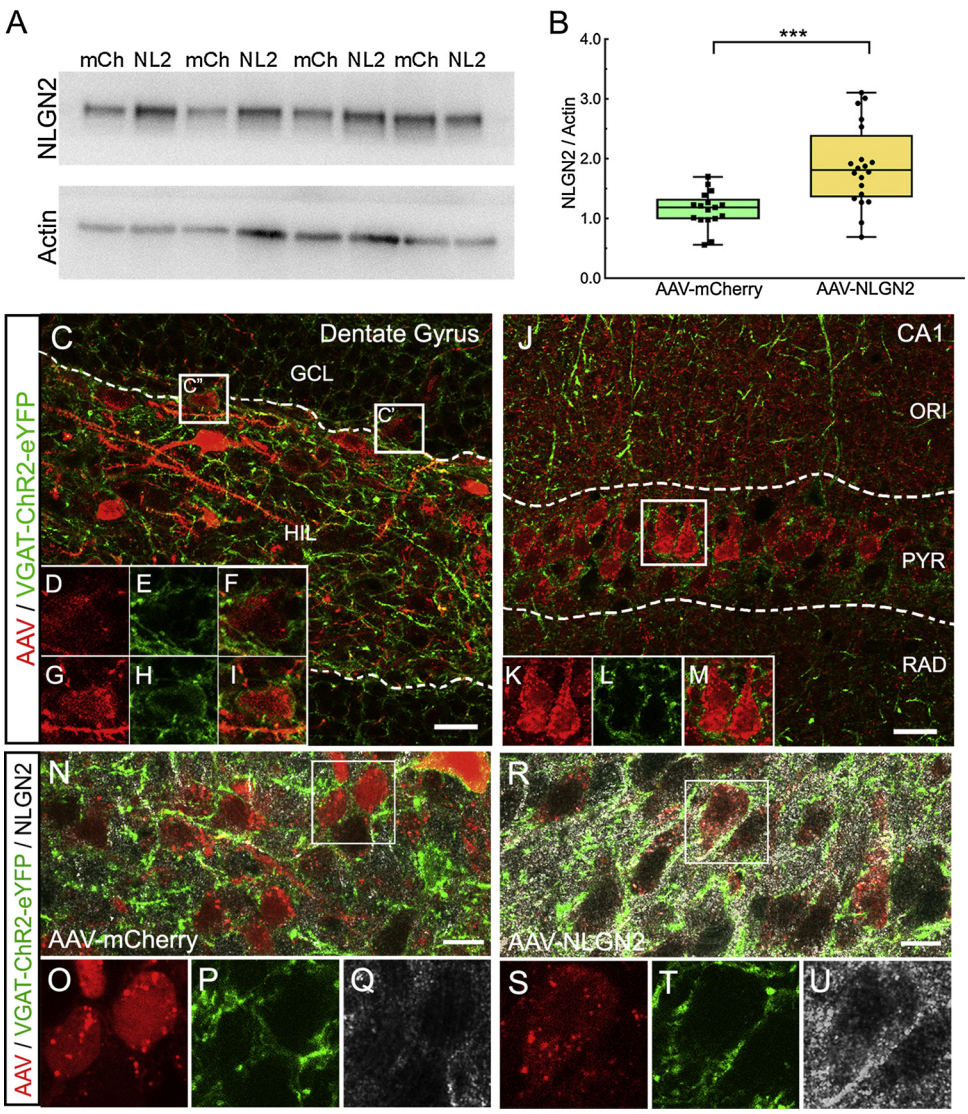

Fig. 1. Increased NLGN2 expression following neuronal transduction with AAV-NLGN2 vector in the adult mouse hippocampus. A, Top panels, representative Western blots showing NLGN2 protein in membrane fractions from hippocampal neurons transduced with the AAV-mCherry vector (mCh) or the AAV-NLGN2 vector (NL2). Beneath, the same blot probed for actin as a loading control. **B,** Box and whisker plot showing average optical density of membranes probed for NLGN2/Actin. Membrane fractions from hippocampus transduced with the AAV-NLGN2 vector contained significantly more NLGN2 protein compared to AAV-mCherry vector controls (***p = 0.0002, Student's t-test). **C–J,** The AAV vectors (red) transduced multiple neuronal cell types in the dentate gyrus (DG). **C**, AAV-transduced GABAergic interneurons (red) in VGAT-ChR2-eYFP (green) transgenic mouse brain showing co-labeling of GABAergic neurons in the hilus (HIL) and granule cell layer (GCL). **D-F**, Magnified views indicated in boxed region in **C'**. **E**, AAV-mCherry transduced GC receiving GABAergic synaptic contacts (green) and **F,** the merged image of this cell. **G-I**, Higher-magnification views indicated in boxed region in **C''**. **G**, AAV-transduced GABAergic interneuron (red) and **H**, VGAT-ChR2-eYFP co-expression (green). **I,** the merged view of cell. **J,** AAV-NLGN2- vector transduced CA1 pyramidal neurons. Labeled neurons in the *stratum pyramidale* (PYR) with dendrites extending into *stratum oriens* (ORI). **K–M,** AAV-mCherry$^+$ pyramidal cells (box) receiving VGAT-ChR2-eYFP labeled synaptic contacts. **K**, mCherry; **L**, eYFP, **M**, merged image. **N-U**, Triple-labeled CA3 pyramidal neuron with **O**, vector driven expression of mCherry (red). **P**, EYFP$^+$ GABAergic inputs on this neuron (green). **Q**, Punctate cell-surface immunostaining for Neuroligin2 (NLGN2, white). **R,** Triple-labeled neurons in a mouse transduced with the AAV-NLGN2 vector; CA1 pyramidal neurons (red) expressed high levels of NLGN2 (white), in association with GABAergic synapses (VGAT-ChR2-eYFP positive boutons; green). Boxed region magnified in **S-U**. **S**, mCherry-labeling; **T**, eYFP$^+$ GABAergic terminals; **U**, NLGN2-immunoreactive puncta. **C, J** Scale bars equal 20 μm; **N, R** scale bars equal 10 μm.

alignment.

2.9. Statistical analysis and graphs

Statistical analyses were performed in the Statistical Package for Social Science (SPSS)(IBM). The graphs were generated in Graph Pad Prism (https://www.graphpad.com/scientific-software/prism/). Box and whisker plots show the maximum and minimum values, with the upper and lower bounds of the box encompassing the third and first quartiles, respectively. All data points are shown on each box and whisker plot. Further information regarding statistical analyses is available in Table S2.

3. Results

3.1. AAV/DJ vector-mediated NLGN2 gene expression increases NLGN2 in the hippocampus

Western blot experiments confirmed that neuronal transduction with the AAV-NLGN2 vector significantly increased levels of NLGN2 in membrane fractions by approximately 55% (Fig. 1A), compared to the AAV-mCherry vector (Fig. 1B; p = 0.0002, Student's t-test; n = 18 hippocampi from 9 AAV-mCherry$^+$ mice, 20 hippocampi from 10 AAV-NLGN2$^+$ mice).

To determine whether the AAV/DJ vector was transduced in both excitatory and inhibitory neurons, we injected the AAV-mCherry or the AAV-NLGN2 vectors into the hippocampus of transgenic mice expressing VGAT-ChR2-eYFP to identify GABAergic interneurons based on green fluorescence. As shown in Fig. 1C–I, GABAergic interneurons in the hilus and the molecular layer (MOL) of the DG were transduced by the vectors, as well granule cells in the DG granule cell layer (GCL), and spiny (putative) mossy cells in the hilus of DG (Fig. 1C–M) and CA1 pyramidal neurons, based on the location of the cell bodies, their morphology, and the presence of punctate GABAergic terminals covering the somas (Fig. 1J–M). Additionally, we found that neurons transduced with AAV-mCherry vector had lower immunoreactivity for NLGN2 (Fig. 1N–Q) compared to neurons transduced with the AAV-NLGN2 vector (Fig. 1R–U). These experiments confirmed that the vectors transduced the principal cells of the hippocampus as well as hippocampal GABAergic interneurons. Moreover, AAV-NLGN2 vector transduction resulted in substantial increases in the expression of the NLGN2 protein in hippocampal neurons.

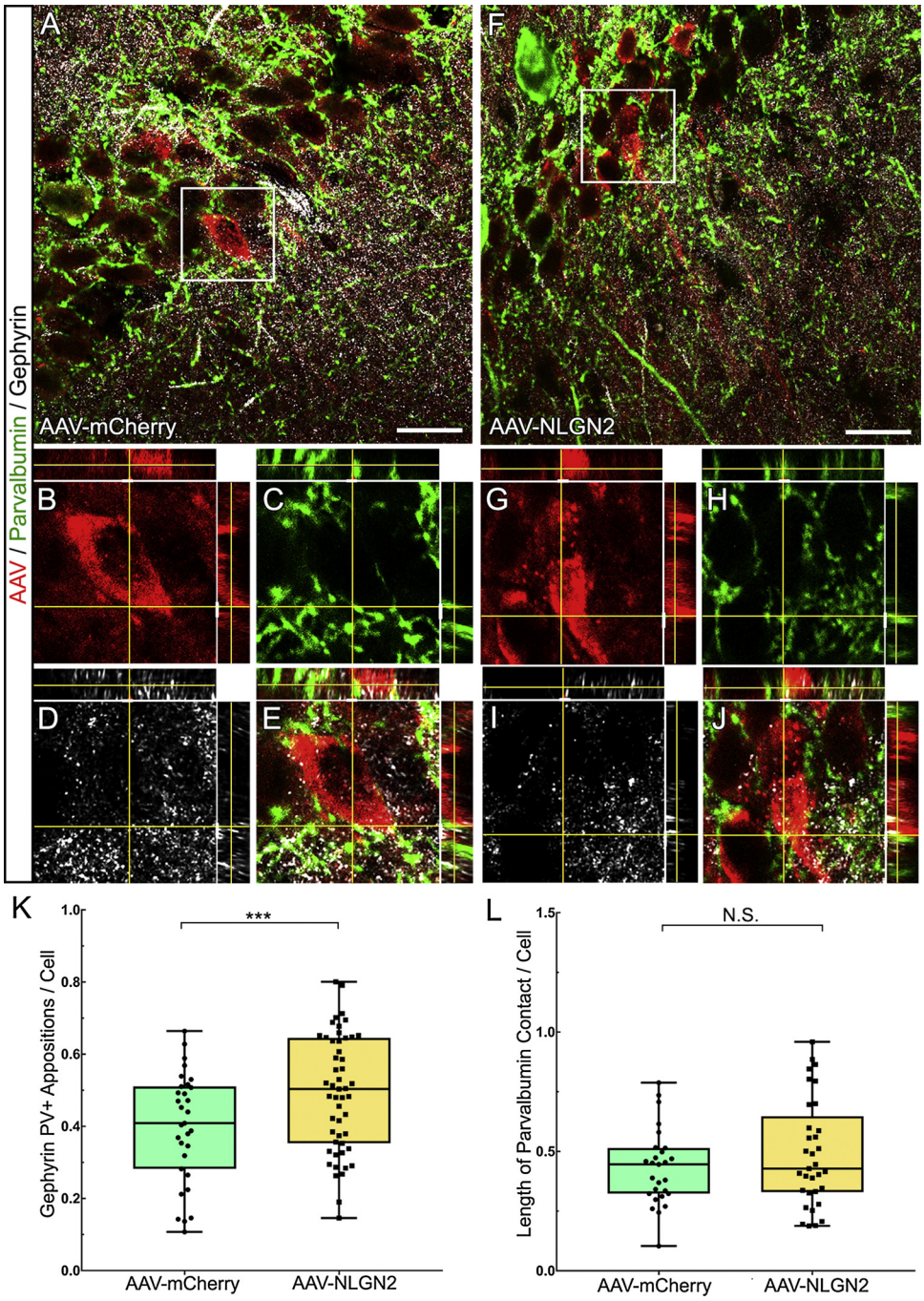

Fig. 2. Increased gephyrin$^+$ synaptic puncta at parvalbumin$^+$ synaptic endings in AAV-NLGN2-expresing neurons. A, CA1 pyramidal neurons (red) transduced with control AAV that were contacted by inhibitory neurons co-expressing parvalbumin (PV$^+$) (green) exhibited sparse gephyrin puncta (white). **B–E,** Higher magnified views of the mCherry$^+$ neuron from **A**, with orthogonal views in the Z-plane. Crosshairs indicate a putative synaptic site where mCherry (**B**), PV (**C**), and gephyrin (**D**) all colocalize (*E*). **F,** CA1 pyramidal neurons (red) infected with experimental AAV-NLGN2 virus that were contacted by PV$^+$ (green) inhibitory interneurons exhibited increased density of punctate gephyrin (white). **G–J,** Higher resolution view of an mCherry$^+$ neuron from **F**, with orthogonal views in the Z-plane. Crosshairs indicate a putative synaptic site where mCherry (**G**), PV (**H**), and gephyrin (**I**) all colocalize in the same z-axis (*J*). **K,** Gephyrin puncta that co-localized with PV$^+$ contacts to AAV-NLGN2- neurons were significantly increased (***p = 0.01, Student's t-test). **L,** The length of PV$^+$ contacts onto AAV-labeled pyramidal cells was unaltered by AAV-NLGN2 (p = 0.26, Student's t-test). Scale bars equal 20 μm.

3.2. Increased gephyrin$^+$ and VGAT$^+$ puncta at putative GABAergic synaptic sites in neurons transduced with AAV-NLGN2

Prior work has established the parvalbumin-expressing (PV$^+$) GABAergic interneurons form inhibitory synapses preferentially at perisynaptic sites containing NLGN2 homomeric dimers. This is in contrast to somatostatin-expressing (SOM$^+$) interneurons, which form NLGN2-NLGN3 heterodimers at synaptic contacts [47]. These prior findings suggested that neurons overexpressing NLGN2 might show increased PV$^+$ GABAergic synapses. To investigate whether transduction with AAV-NLGN2 led to an increase in PV$^+$ GABAergic synapses, we utilized immunostaining and high-resolution confocal microscopy. We addressed this question by quantifying putative synaptic boutons expressing PV$^+$ that co-localized with postsynaptic gephyrin$^+$ puncta in virally-transduced hippocampal neurons (Fig. 2A–J). Overall, we found a 23% increase in PV$^+$ synaptic endings aligned with gephyrin$^+$ puncta in AAV-NLGN2$^+$ pyramidal neurons, compared to neurons transduced with AAV-mCherry (Fig. 2K; AAV-NLGN2$^+$ neurons: 20.27 ± 1.22 PV$^+$/gephyrin$^+$ puncta/cell vs. AAV-mCherry$^+$ neurons: 16.48 ± 1.20 puncta/cell, p = 0.04, Student's t-test). Similarly, by counting the number of PV$^+$/gephyrin$^+$ appositions per micron of labeled cell membrane; we found ~23% more appositions per micron in AAV-NGLN2$^+$ neurons (0.49 appositions/μm) compared to AAV-mCherry$^+$ neurons (0.40 appositions/μm; data not shown; p = 0.01, Student's t-test; n = 31 cells from 4 AAV-mCherry$^+$ control mice and 51 cells from 5 AAV-NGLN2$^+$ mice). However, the lengths of contacts between PV$^+$ axons and AAV-NLGN2$^+$ pyramidal neurons was not significantly different from controls (Fig. 2L; p = 0.26, Student's t-test; n = 27 cells from 4 AAV-mCherry$^+$ mouse brains and n = 33 cells from 5 AAV-NLGN2$^+$ brains). These results suggest that transduction with

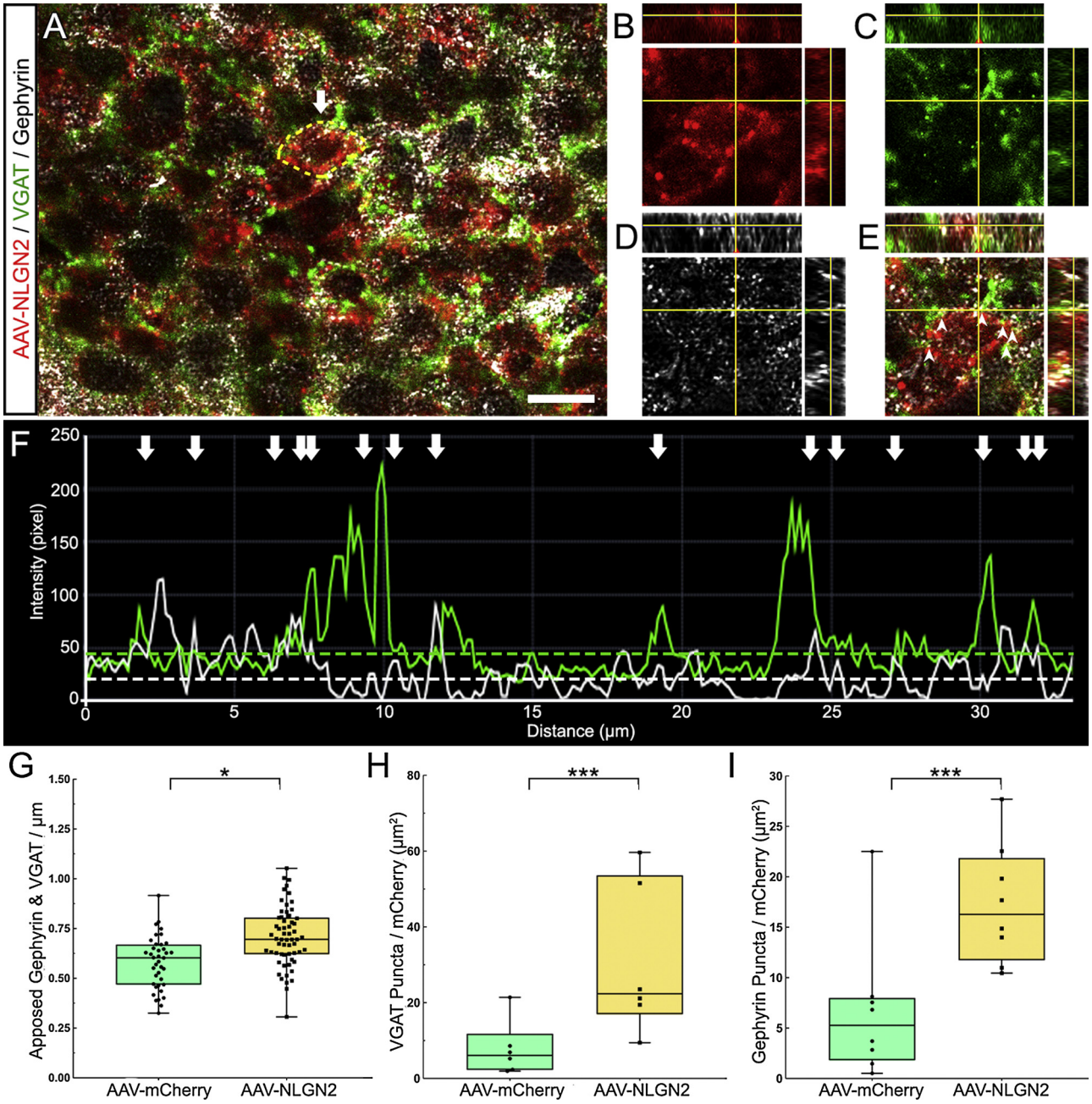

Fig. 3. AAV-NLGN2 expression increased gephyrin-immunoreactive puncta at putative GABAergic synapses. A, AAV-NLGN2$^+$ GCs (red) with presynaptic VGAT (green) and postsynaptic gephyrin (white) immunoreactivity. **B–D,** A representative GC (yellow dashed line, arrow) is shown with co-localization of immunoreactivity for mCherry (red), VGAT (green), and gephyrin (white) in X, Y, and Z-axes in confocal Z-stacks. **E,** Merged image of cell from B–D, **F,** Representative fluorescence histogram generated from the GC shown in B–E. For this cell, the VGAT immunofluorescence is represented by the green histogram, the gephyrin immunofluorescence is represented by the white histogram, and the dashed lines indicate baseline values. Arrows indicate sites along the membrane where peaks of fluorescence detected for presynaptic VGAT and postsynaptic gephyrin were above baseline levels and colocalized, indicating putative pre and postsynaptic sites. **G,** Quantification of putative pre- and postsynaptic sites using histogram analyses showed that AAV-NLGN2$^+$ cells had significantly more apposed VGAT and gephyrin (*p = 0.0003, Student's t-test). **H,** AAV-NLGN2$^+$ cells also had significantly also significantly more VGAT puncta per µm^2 of mCherry (***Student's t-test, p = 0.0057). **I,** AAV-NLGN2$^+$ cells had significantly more gephyrin puncta per µm^2 of mCherry (***Student's t-test, p = 0.0195). **A–D, E**; Scale bars equal 20 µm.

the AAV-NLGN2 vector resulted in high expression of NLGN2 in hippocampal neurons and increased trafficking of inhibitory postsynaptic proteins to sites of parvalbumin$^+$ GABAergic synapses, in agreement with previous in vitro studies [3,15,17].

The finding that AAV-NLGN2 transduction led to a preponderance of PV$^+$/gephyrin$^+$ putative synapses led us to next ask whether AAV-NLGN2 led to a significant increase in GABAergic synapses. To address this, we identified putative GABAergic synapses onto virally transduced neurons. As shown in Fig. 3(A, B), AAV-NLGN2$^+$ neuronal cell bodies and proximal dendrites (identified by mCherry expression) were outlined by VGAT$^+$ GABAergic synaptic boutons (Fig. 3C). Many of these putative presynaptic boutons co-localized with postsynaptic gephyrin$^+$ puncta in neurons transduced with the AAV (Fig. 3D, E, arrowheads). Based on counts of sites with co-alignment of VGAT$^+$ boutons and gephyrin$^+$ puncta (VGAT$^+$ /gephyrin$^+$ puncta, Fig. 3F, arrows), AAV-NLGN2$^+$ neurons showed significantly more co-localized puncta (21.769 ± 0.5829 in n = 52 AAV-NLGN2$^+$ neurons) as compared to controls (16.897 ± 0.5771 co-localized puncta in n = 39 AAV-

mCherry$^+$ neurons) ($p = 0.0000001$; Student's t-test). To control for possible sampling biases, we also analyzed the density of co-labeled puncta per micron of cell surface and found that, on average, AAV-NLGN2$^+$ neurons had 0.69 VGAT$^+$ /gephyrin$^+$ puncta /μm whereas AAV-mCherry$^+$ neurons had approximately 0.58 VGAT$^+$/gephyrin$^+$ puncta/μm (Fig. 3G; $p = 0.0003$, Student's t-test; $n = 39$ neurons from 3 AAV-mCherry$^+$ control mice and 52 neurons from 5 AAV-NLGN2$^+$ mice). Taken together, these findings suggest that AAV-NLGN2 transduction substantially increased putative GABAergic synapses containing gephyrin, a key postsynaptic inhibitory protein responsible for anchoring GABA receptors and other molecules at the postsynaptic density.

We next asked whether AAV-NLGN2 transduction altered the overall level of VGAT localized to putative GABAergic synaptic terminals, as increased VGAT could resulted in enhanced synaptic release of GABA from vesicular stores. To address this question, we analyzed larger regions of interest (ROI) within the hippocampal subfields, while controlling for variations in AAV transduction, using mCherry expression as a proxy (Fig. 3A and B). We found an increase of ˜39% in the number of VGAT$^+$ puncta (17.26 puncta/μm^2 mCherry expression ± 2.10) in the hippocampus of mice transduced with the AAV-NLGN2 vector, compared to mice injected with the control AAV-mCherry vector (6.69 puncta/μm^2 mCherry expression ± 2.47, Fig. 3L; $p = 0.00057$; Students t-test; $n = 8$ GCL subfields from 3 AAV-mCherry$^+$ mice and 8 GCL subfields from 5 AAV-NLGN2$^+$ mice). Similarly, we found ˜25% increase in the overall density of gephyrin puncta (30.80 puncta/μm^2 mCherry expression ± 8.15), compared to controls (7.76 puncta/μm^2 mCherry expression ± 2.93, Fig. 3M; $p = 0.01$; Student's *t*-test; $n = 8$ GCL sections from 3 AAV-mCherry$^+$ mice and 8 GCL sections from 5 AAV-NLGN2$^+$ mice). Thus, transducing hippocampal neurons with the AAV-NLGN2 vector not only increased recruitment, retention or membrane trafficking of gephyrin but also had transynaptic effects by increasing VGAT.

3.3. AAV-NLGN2 transduction is linked to elevated levels of GABAergic synaptic proteins

Prior studies showed that a key role of NLGNs is to provide a linkage between the extracellular and intracellular proteins at synapses [8,18,48,49] and our results support this view by showing that NLGN2 overexpression increased NLGN2, VGAT, and gephyrin at putative GABAergic synapses. As VGAT specifically localizes to GABAergic synaptic vesicles, and gephyrin localizes to the postsynaptic specialization at GABAergic synapses, our findings could indicate that AAV-NLGN2's effects include increasing or enhancing efficacy of GABAergic synaptic transmission, however testing this hypothesis would require either quantitative immuno-electron microscopic studies or electrophysiology or both. As an alternative, we chose a biochemical approach to compare the extent of membrane recruitment of inhibitory synaptic proteins VGAT, gephyrin, and the $GABA_A$ receptor-specific $GABA_AR\gamma2$ subunit [50,51] in mice transduced with either the AAV-NLGN2 vector or the AAV-mCherry vector (Fig. 4A). AAV-NLGN2 transduction significantly increased hippocampal membrane-associated gephyrin by 1.3-fold (Fig. 4B; $p = 0.0326$, Student's t-test; $n = 18$ hippocampi from 9 AAV-mCherry$^+$ mice and $n = 20$ hippocampi from 10 AAV-NLGN2$^+$ mice). Similarly, AAV-NLGN2 transduction significantly increased VGAT in membrane fractions ˜1.5-fold increase (Fig. 4C; $p = 0.0097$, Student's t-test; $n = 18$ hippocampi from 9 AAV-mCherry$^+$ mice and 20 hippocampi from 10 AAV-NLGN2$^+$ mice). Moreover, overexpression of NLGN2 increased membrane levels of the GABA receptor subunit, $GABA_A\gamma2$ by ˜2.1-fold (Fig. 4D; $p = 0.016$, Student's t-test; $n = 8$ hippocampi from 4 AAV-mCherry$^+$ mice, 10 hippocampi from 7 AAV-NLGN2$^+$ mice).

3.4. AAV-NLGN2 vector transduction did not increase excitatory synaptic proteins

Our results showing that AAV-NLGN2 transduction increased levels of inhibitory synaptic proteins in hippocampal synaptic membranes, led us to ask whether these effects were specific for proteins normally trafficked to GABAergic synapses. To address this, we assayed whether AAV-NLGN2 transduction increased excitatory synapse-specific proteins at putative synaptic sites in neuronal membranes [13,52–55]. As shown in Fig. 5(A–F) vesicular glutamate transporter (vGlut) immunoreactive puncta were localized on the surfaces of apical dendrites of pyramidal neurons and on somas. When we quantified excitatory synapses onto pyramidal neurons and dentate GCs, we found that the density of vGlut$^+$ puncta did not differ between neurons transduced with AAV-NLGN2 or AAV-mCherry (Fig. 5G; 15.81 puncta/μm mCherry expression ± 3.26 in $n = 5$ AAV-NLGN2$^+$ mice vs. 13.09 puncta/μm mCherry expression ± 2.34 $n = 3$ AAV-mCherry$^+$ control mice; Students *t*-test, $p = 0.56$).

To further extend these immunohistochemical data, we next used biochemical approaches to examine levels of the excitatory postsynaptic density protein 95 (PSD95) and N-Methyl-D-aspartate receptor (NMDA) subunit NR2B protein in membrane fractions from the hippocampus of mice receiving AAV-NLGN2 vector vs. the control vector (Fig. 5H). Neither the level of PSD95 (Fig. 5I; $p = 0.33$, Student's t-test; $n = 16$ hippocampi from AAV-NLGN2$^+$ mice vs. $n = 13$ hippocampi from AAV-mCherry$^+$ control mice) nor NR2B differed (Fig. 5J; $p = 0.35$, Student's t-test; $n = 9$ hippocampi from AAV-NLGN2$^+$ mice vs. $n = 7$ hippocampi from AAV-mCherry$^+$ control mice). These results suggest that AAV-NLGN2 vector transduction of hippocampal neurons selectively increased GABAergic synaptic proteins, but not excitatory synaptic proteins.

3.5. NLGN2 overexpression in the hippocampus is associated with altered social dominance and social preference

Our finding that NLGN2 increased putative GABAergic synapses led us to examine the effects on behavior. We first tested for social dominance and compared wins and losses of experimental mice receiving hippocampal injections of the AAV-NLGN2 vector when they were matched against control mice receiving hippocampal injections of the AAV-mCherry vector (Fig. 6A). Our initial analysis, using Fisher's exact test, indicated that group scores were significantly different than what would be expected by chance ($p = 0.02$). Next, we constructed a 95% confidence interval to analyze score distributions in bouts between groups. AAV-NLGN2$^+$ mice had an upper confidence bound of 0.4881, which skewed their group results significantly below the 0.5 chance score. Comparatively, control mice with AAV-mCherry vector transduction showed a lower confidence interval of 0.6, indicating a win value of greater than chance (1-sample t-interval test). Direct comparisons of wins/bouts between groups showed that mice with AAV-NLGN2 transduction had significantly lower dominance ratios (Fig. 6B; $p < 0.01$, Student's t-test; $n = 18$ AAV-mCherry$^+$ and 24 AAV-NLGN2$^+$ mice).

We next compared social preference and social memory for conspecific mice with the three-chambered sociability test (Fig. 6C). In the test of preference for a novel object versus a novel mouse, both AAV-NLGN2$^+$ and AAV-mCherry$^+$ animals showed a preference for social interaction, with no significant differences between groups (data not shown; $p = 0.84$, Student's t-test). When comparing preference for social novelty, as expected, control mice exhibited normal novelty preference and spent significantly more time with a novel mouse than the familiar one ($p < 0.01$, Student's t-test; $n = 20$). In contrast, AAV-NLGN2$^+$ mice did not spend more time with the novel vs. familiar mouse ($p = 0.25$, Student's t-test; $n = 24$). Similarly, the novelty discrimination index was significantly greater for control vs. AAV-NLGN2$^+$ mice (discrimination index = time with novel mouse – time

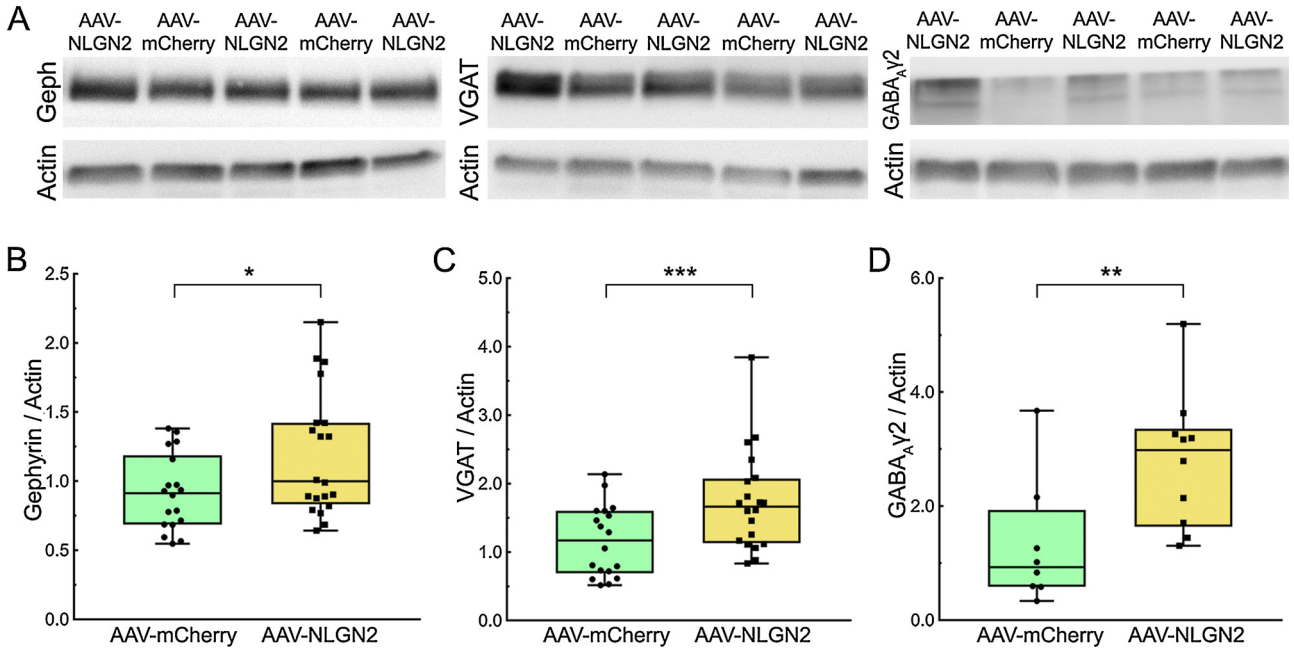

Fig. 4. GABAergic synaptic proteins gephyrin, VGAT and $GABA_A\gamma2$ were significantly increased after transduction of hippocampal neurons with AAV-NLGN2. A, Western blots showing bands for gephyrin, VGAT, $GABA_A\gamma2$, and actin in hippocampal membrane fractions from mice receiving stereotaxic injections of the AAV-NLGN2 or AAV-mCherry vectors into the hippocampus. **B,** Total membrane levels of gephyrin were significantly increased after transduction with the AAV-NLGN2 vector, compared to the AAV-mCherry vector ($p = 0.032$, Student's t-test). **C,** Total membrane levels of VGAT protein were significantly increased after transduction with the AAV-NLGN2 vector, compared to the AAV-mCherry vector ($p = 0.0097$, Student's t-test). **D,** Total membrane levels of $GABA_A\gamma2$ were significantly increased after transduction with AAV-NLGN2, compared to the AAV-mCherry vector ($p = 0.016$, Student's t-test).

with familiar mouse/total interaction time) (Fig. 6D; $p = 0.03$, Student's t-test).

3.6. NLGN2 overexpression in the hippocampus does not alter anxiety

Given that the hippocampus and amygdala are highly interconnected, we reasoned that hippocampal NLGN2 overexpression might impact anxiety-like behaviors, as assessed in the Open Field test and elevated Zero Maze (Fig. 6E). In the Open Field, both AAV-NLGN2$^+$ and AAV-mCherry$^+$ mice did not differ significantly in time spent in the center of the arena (182.34 ± 12.02 s in n = 16 AAV-mCherry$^+$ controls vs. 182.32 ± 14.26 s in n = 17 AAV-NLGN2$^+$; $p = 0.99$, Student's t-test). Distance travelled was also equivalent (65.82 ± 3.50 m in AAV-mCherry$^+$ mice, 62.83 ± 2.97 in AAV-NLGN2$^+$ mice; $p = 0.52$, Student's t-test). We also found no significant differences in the time spent in the open arms of the Zero Maze (Fig. 6F; 39.96 ± 7.5 s in n = 13 AAV-mCherry$^+$ controls vs. 37.96 ± 6.51 s in n = 17 AAV-NLGN2$^+$ mice; $p = 0.84$, Student's t-test). Furthermore, the experimental and control animals travelled the same distance; AAV-mCherry$^+$ mice travelled on average 10.34 ± 1.16 m vs. AAV-NLGN2$^+$ mice which travelled 9.05 ± 0.82 m, suggesting equivalent motor activity levels ($p = 0.36$, Student's t-test). Therefore, our data suggest that mice with hippocampal transduction of AAV-NLGN2 do not show increased anxiety, compared to AAV-mCherry$^+$ controls.

3.7. NLGN2 overexpression correlates with disruptions in hippocampal-dependent spatial memory

GABAergic inhibitory interneurons fine tune spatial memory in the hippocampus and entorhinal cortex [31,35,56,57]. An altered excitatory/inhibitory balance in the hippocampus could disrupt the ability to form normal place fields. To determine whether AAV-NLGN2 induced enhancement of hippocampal GABAergic synapses correlated with altered spatial memory performance, we evaluated memory using the novel object location test and the Morris water maze. In the novel object location test, a mouse must recognize that one of two previously known objects has been displaced from its original location (Fig. 7A). On average, controls spent 33.4 s longer with the novel-located object, whereas AAV-NLGN2$^+$ animals only spent 4.8 s longer with the novel object. When expressed as a discrimination index for novelty, mCherry controls showed a significantly higher discrimination index for novelty compared to AAV-NLGN2$^+$ mice (Fig. 7C; $p < 0.01$, Student's t-test; n = 13 AAV-mCherry$^+$ control mice vs. n = 13 AAV-NLGN2$^+$ mice).

To confirm that the cognitive deficits were not due to impaired vision or novelty preferences, we compared performance in the novel object recognition test. This task requires that the mice distinguish between a familiar and unfamiliar object after an hour of memory consolidation. We found that both AAV-NLGN2$^+$ and control animals showed a significantly greater preference for the novel object compared to the familiar one (Fig. 7B; $p < 0.01$ AAV-NLGN2$^+$ mice vs. $p < 0.05$ AAV-mCherry$^+$ control mice; Student's t-test) with similar discrimination indices for novelty (Fig. 7D; $p > 0.05$, Student's t-test; n = 13 AAV-NLGN2$^+$ mice and n = 13 AAV-mCherry$^+$ control mice). Taken together, these findings suggest that transducing hippocampal neurons with the AAV-NLGN2 vector resulted in mnemonic deficits.

To further examine hippocampal-dependent spatial memory deficits, we tested these two groups of mice in the Morris water maze (Fig. 7E). Control mice showed normal, average escape latencies under 15 s for all three days of uncued learning, while the AAV-NLGN2$^+$ mice were significantly worse (Fig. 7F; $p < 0.05$, two-way repeated measures ANOVA). In the probe trial, AAV-NLGN2$^+$ mice showed a non-significant trend towards longer latencies for crossing the platform area (Fig. 7G; $p = 0.08$, Student's t-test) and crossed through the platform area significantly fewer times, compared to controls (Fig. 7H $p = 0.02$, Student's t-test; n = 12 AAV-mCherry$^+$ control mice vs. 16 AAV-NLGN2$^+$ mice). However, quadrant dwell time in the probe trial was unaffected by NLGN2 overexpression, with both groups spending significantly more time in the target quadrant compared to the opposite quadrant ($p > 0.05$, ANOVA). Deficits in learning could not be correlated with motor or visual impairments, as both groups performed

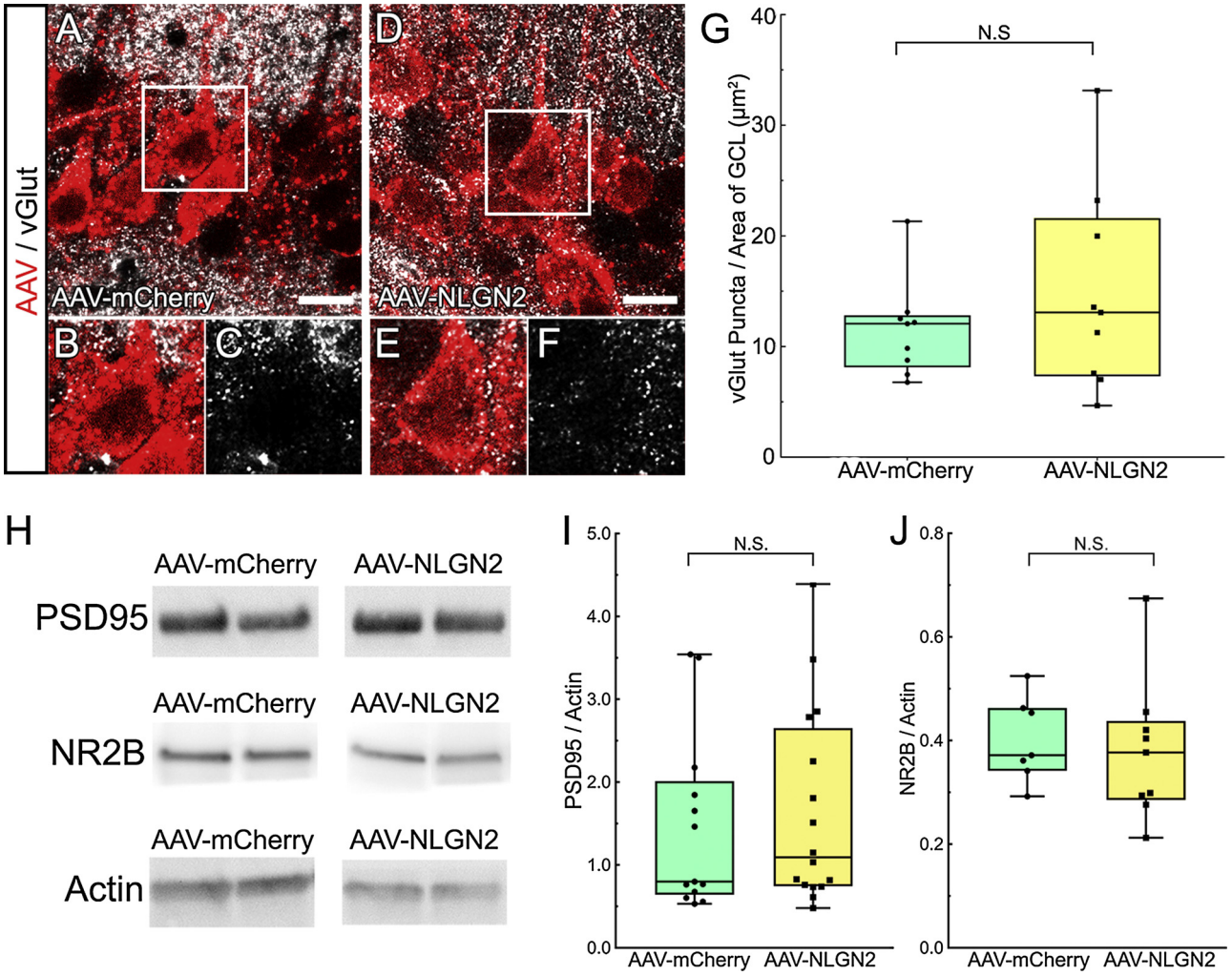

Fig. 5. Excitatory synaptic proteins vGlut, PSD-95, and NR2B were not altered after transduction of hippocampal neurons with AAV-NLGN2. A, Representative confocal photomicrographs showing putative sites of synaptic contacts indicated by vGlut$^+$ puncta (white) on AAV-mCherry$^+$ pyramidal neurons (red). **B, C,** Magnified views of selected cells. **D,** Confocal images of vGlut$^+$ puncta (white) apposed to AAV-NLGN2$^+$ pyramidal neurons (red). **E, F,** Magnified views of selected cells. **G,** Quantification for vGlut$^+$ puncta/µm^2 of mCherry immunofluorescence showing that vGlut$^+$ puncta were not increased in neurons transduced with the AAV-NLGN2 vector, compared to AAV-mCherry vector ($p = 0.5631$, Student's t-test). **H,** Representative Western blots comparing PSD95 and NR2B protein bands in hippocampal membrane fractions after transduction with the AAV-NLGN2 or the AAV-mCherry vectors. **I,** Quantification of protein bands revealed that PSD95 was not significantly different in the tissue transduced with the two different vectors ($p = 0.6622$, Student's t-test). **J,** Membrane levels of NR2B were also comparable in hippocampal tissue transduced with the AAV-NLGN2 or AAV-mCherry vectors ($p = 0.7113$, Student's t-test). **A, D,** Scale bars equal 20 µm.

identically when they were tested in cued learning trials with a visible, marked platform (Fig. 7F). Taken together, these results suggest that AAV-NLGN2$^+$ mice showed significant cognitive impairments in hippocampal-dependent tasks, including social dominance, social memory, and some measures of performance in spatial memory, while performing normally on tests of anxiety, motor behavior, and visually cued learning.

4. Discussion

Previous *in vitro* studies showed that NLGN2 recruits synaptic proteins to synaptic locations [15,17,58] in accordance with *in vivo* studies suggesting that NLGN2 is critical in assembling components of GABAergic synapses [3,8,18,59,60]. Studies in adult mice examining the effects of altered NLGN2 expression on behavior have given conflicting results. However, mutations in synaptic adhesion molecules in human patients, including the NLGN family, are commonly associated with neuropsychiatric disorders [61–63]. Mutations in NLGN3 and NLGN4 are well characterized in autism patients [10,64] and recent case studies in schizophrenia and autism patients have linked missense mutations in NLGN2 to disease phenotypes [9,12]. While prior studies investigated mRNA expression following experimentally-increased NLGN2 [25], our work is the first to examine whether NLGN2 overexpression increased localization of GABAergic synaptic proteins at inhibitory synapses. We utilized viral-mediated gene delivery to overexpress NLGN2 in the adult mouse dentate gyrus and CA1-CA3 regions of the hippocampus and quantified the number of PV$^+$ GABAergic synaptic endings apposed to gephyrin puncta in neurons expressing NLGN2 by confocal microscopy.

Our results show that AAV-NLGN2 transduction in adult hippocampal neurons increased putative GABAergic synapses in the adult mouse dentate gyrus and CA1. NLGN2 overexpression resulted in a significant increase at putative GABAergic terminals in VGAT and gephyrin, a molecule localized to the postsynaptic scaffold at GABAergic synapses. Both VGAT, the presynaptic vesicular transporter that packages GABA [65] and gephyrin, a protein essential to postsynaptic $GABA_AR$ clustering [50,66,67] are necessary components of the GABAergic synapse, and their appositions are most likely found at GABAergic synapses, although definitive proof would require additional electron microscopic studies. Our results do suggest however, that AAV-

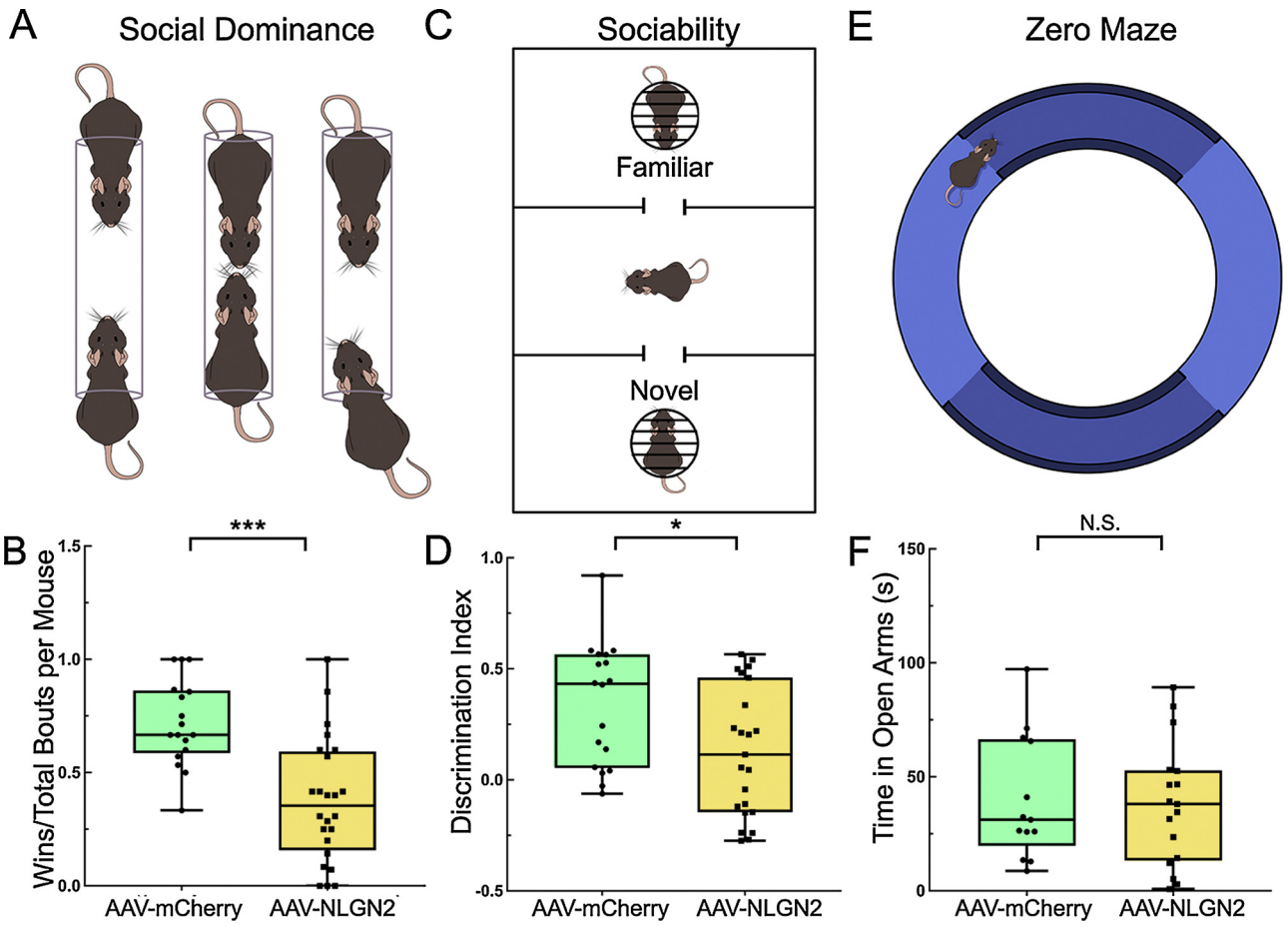

Fig. 6. Altered social behavior but not anxiety following neuronal transduction with the AAV-NLGN2 vector. A, Schematic of the tube test apparatus for investigating social dominance. **B,** Mice transduced with the AAV-NLGN2 vector showed reduced dominant aggressive behavior compared to mice transduced with the AAV-mCherry vector (***$p < 0.01$, ANOVA). **C,** Schematic of the three-chambered sociability test apparatus. **D,** Mice transduced with the AAV-NLGN2 vector showed reduced preference for novel interactions (discrimination index), compared to controls ($p = 0.0201$, Student's t-test). E, Schematic of the elevated zero maze apparatus. **F,** Mice transduced with the AAV-NLGN2 vector showed anxiety levels comparable to AAV-mCherry transduced mice, based on time spent in the open arms of the zero maze ($p = 0.8420$, Student's t-test).

NLGN2 may increase inhibitory neurotransmission in the adult hippocampus by recruiting molecules involved in neurotransmitter uptake in presynaptic vesicles and GABAergic receptor trafficking.

Our results expand upon a previous biochemical study that examined genetic overexpression of NLGN2 in mice; this prior study demonstrated increased VGAT, syntaxin, and NLGN3, but they did not examine different brain regions, nor did they analyze neuronal membrane fractions, where synaptic proteins are localized [21]. Our Western blot analyses of gephyrin, VGAT, and $GABA_AR\gamma2$, the gephyrin-associated $GABA_A$ subunit [51,68,69], demonstrated that mice receiving the AAV-NLGN2 vector showed significant increases in GABAergic synapse-specific molecules in hippocampal membrane fractions, compared to controls. The accumulation of $GABA_AR\gamma2$ with AAV-NLGN2 overexpression may be due to increased $GABA_A$ receptor trafficking to synaptic sites and/or reduced endocytosis and these possibilities should be investigated in future studies. We did not find an effect of AAV-NLGN2 on excitatory synaptic proteins, suggesting that NLGN2 overexpression-induced changes are specific to GABAergic synapses. Thus, at least after 3–4 weeks, AAV-NLGN transduction increased recruitment or expression of GABAergic synaptic molecules, without concomitant changes in excitatory synaptic proteins.

Our results showing an increase in both structural and functional components of GABAergic synapses with NLGN2 overexpression concur with a previous genetic knockout study demonstrating that NLGN2 deficiency reduced $GABA_AR\gamma2$ and gephyrin clustering and also increased neuronal excitation [70]. Thus, NLGN2 overexpression might increase inhibitory postsynaptic currents in mature neurons or the quantal release of GABA, and it would be of interest to directly test this in future studies.

An important area for future work would be to determine how NLGN2 overexpression alters the functional properties of hippocampal circuits. Our AAV/DJ vector transduced excitatory granule cells, pyramidal cells, putative hilar mossy cells, and inhibitory GABAergic interneurons. Further electrophysiological studies are required to dissect apart the effects of altering GABAergic neurotransmission onto different hippocampal cell types. This brain region contains multiple subtypes of interneurons, including some that specifically target and inhibit other GABAergic interneurons, causing disinhibition [71–73]. NLGN2 overexpression in these cells could lead to disinhibition which might cause cognitive deficits and altered social behavior. Alternatively, NLGN2 overexpression in interneurons could enhance excitation, as suggested by a recent study of the long-range GABAergic projections from the parvalbumin$^+$ interneurons in the entorhinal cortex, which are regulated by NLGN2 homomeric dimers [47] and serve an excitatory rather than inhibitory role in the hippocampus [74]. Therefore, limiting NLGN2 overexpression to subsets of GABAergic or glutamatergic neuron populations using an intersectional approach could provide additional insights into NLGN2's role in regulating different types of GABAergic synapses and the effects on behavior and cognition.

Considering the role of GABAergic interneurons in hippocampal-

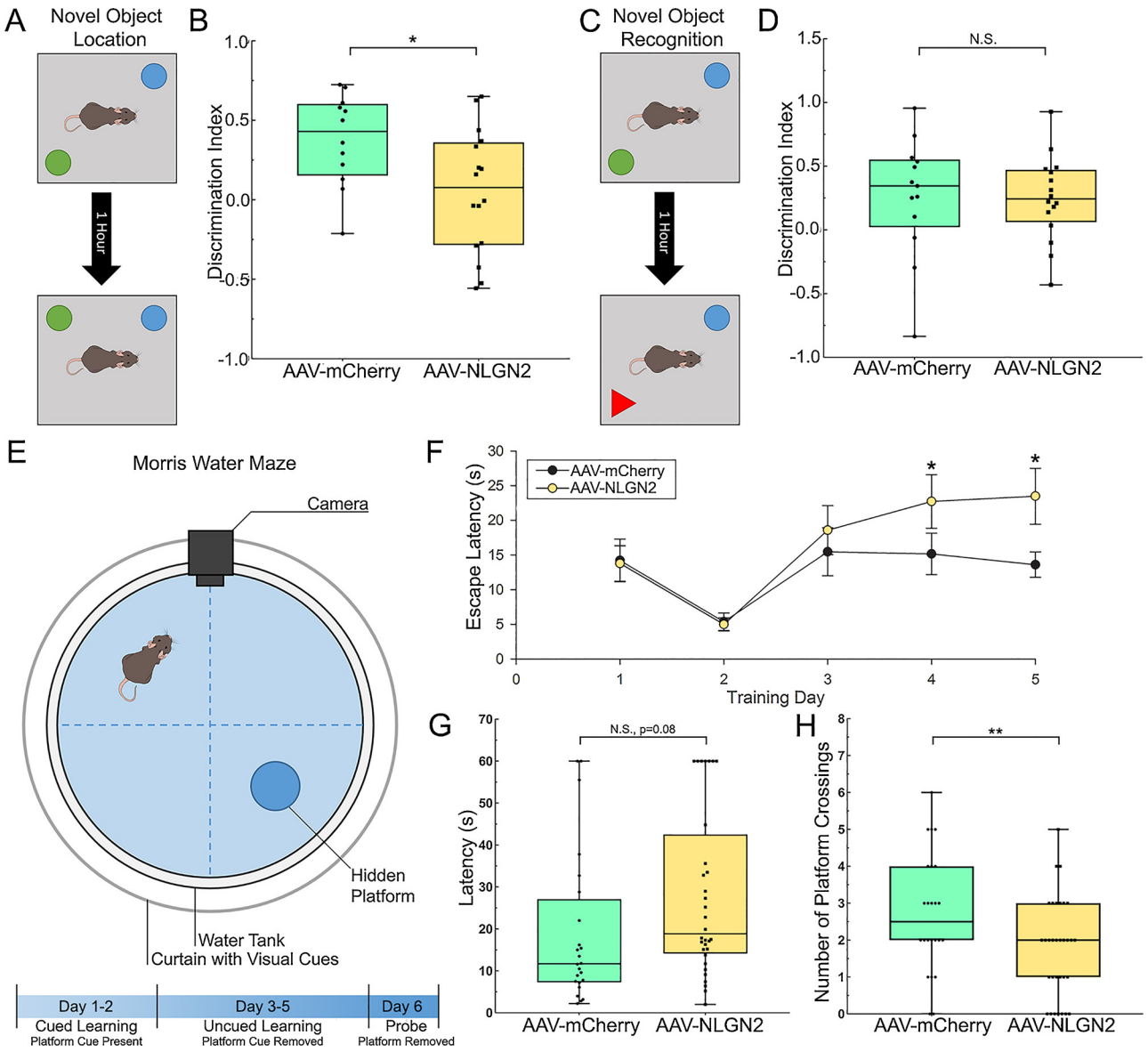

Fig. 7. Impaired performance in spatial memory tasks but not in tasks that did not depend upon the hippocampus following neuronal transduction with the AAV-NLGN2 vector. A, Schematic of the apparatus used for testing recall of a novel object's location. **B,** Mice transduced with the AAV-NLGN2 vector showed reduced discrimination between objects in the same vs. novel locations, compared to mice that were transduced with the AAV-mCherry vector ($p = 0.0358$, Student's t-test). **C,** Schematic of the apparatus for testing hippocampal-independent novel object recognition. **D,** Mice showed a similar preference for the new object, indicating that they were able to recall the previously explored object ($p = 0.9231$, Student's t-test). **E,** Schematic and timeline for the Morris water maze test of spatial memory. **F,** Mice transduced with the AAV-NLGN2 or AAV-mCherry vectors performed similarly during cued learning, but the mice transduced with the AAV-NLGN2 vector showed significant impairments in learning the spatial navigation task during days 3–5, after the platform cue was removed ($p = 0.043$, Two-way repeated measures ANOVA). **G,** During probe trials, AAV-NLGN2 transduced mice showed a trend toward longer latencies to initially crossing the platform, compared to AAV-mCherry controls ($p = 0.0815$, Student's t-test). **H,** Mice transduced with the AAV-NLGN2 vector crossed the platform area significantly fewer times than mice transduced with the AAV-mCherry vector ($p = 0.0220$, Student's t-test).

dependent behaviors, increased inhibitory synaptic transmission in the hippocampus in animal models might be predicted to alter social behavior, social dominance, aggression, anxiety, and/or learning and memory. Considerable interest in this topic is supported by studies that have linked the development of autism, comorbid with social deficits, to deficits in members of the NLGN family, particularly NLGN2-4 [9,10,14,61,62,64,75]. Regarding hippocampal-dependent social behaviors, projections between the hippocampus and the amygdala coordinate the formation of emotional contexts necessary for social memory [76], while social behavior and aggression are regulated by multiple regions in the hippocampus, including the dentate, CA1, CA2, and CA3 [29,30,77–83]. Several previous studies examined the effects of NLGN2 overexpression in the hippocampus on novelty preference, anxiety, social behavior, and aggression in both rats and mice, but the results were contradictory [25,27].

To study the effects of overexpressing NLGN2 on social interactions, we used Crawley's three-chambered sociability test and found deficits in preference for social novelty. Our results in mice NLGN2 overexpression throughout the hippocampus are in agreement with a previous study in mice [27]. However, a second study from this group performed in rats with NLGN2 overexpression limited to the dorsal hippocampus failed to show a deficit in preference for social novelty, emphasizing the importance of ventral hippocampal circuits for regulating social behaviors in mice [25].

Conflicting results have also been obtained regarding NLGN2's effect on social dominance or aggressive behavior [25,27,84]. As prior

work had examined aggression in the resident intruder test [30,32], we examined the formation of dominance hierarchies with the tube test of social dominance. This quick, simple and common assay for assessing social dominance behavior in mice has been used extensively for over 50 years [45]. Abnormal tube test dominance behavior is typically observed in mice that display other deficits in social interactions. Importantly, new findings in the present study is that mice with NLGN2 overexpression in the hippocampus show significant changes in social interactions and dominance behavior; mice with AAV-NLGN2 overexpression exhibited reduced dominance in the tube test when matched against the controls. Although they were significantly less likely to push a control mouse out of the tube, they showed normal performance within their treatment group.

In contrast to the effects of overexpressing NLGN2 on social behaviors, we did not find alterations in anxiety-related behaviors, as assessed with the Zero maze or the Open Field test, in agreement with a prior study in which NLGN2 was overexpressed in the rat dorsal hippocampus followed by testing for anxiety in the elevated plus maze [25]. The elevated Zero Maze appears to be more sensitive to changes in GABAergic neurotransmission than the elevated plus maze and studies have reported that performance in the elevated zero maze is relatively stable over several trials whereas mice adapt rapidly to the elevated plus maze over time [41]. Our results are also consistent with prior studies in mice that examined the effects of genetically-induced NLGN2 deficiency and showed that this manipulation increased anxiety-like behaviors, not only in the elevated plus maze, but also in the light-dark box and open field test [28,29]. Taken together, these findings suggest that while NLGN2 may be necessary to establish inhibitory circuits involved in anxiety-related behaviors, increasing NLGN2 above normal levels in the adult brain may not have a measurable effect on anxiety.

Based on a prior study showing deficits in contextual fear memory acquisition following conditional knockout of NLGN2 in the rodent prefrontal cortex [85,86], and work showing deficits in spatial memory in mice expressing the human R215H loss of function mutation in NLGN2 [87], we predicted that AAV-NLGN2-mediated overexpression would significantly alter memory formation. As object investigation in the open field had been studied following NLGN2 overexpression [25], we chose to focus on acquisition of spatial memory in two different paradigms - the Morris Water Maze and the novel object location test, which requires that the mouse distinguish between an object in a familiar location and that same object after it is moved to a new location [88–90]. When compared with controls, the mice with NLGN2 overexpression showed impairments in their ability to discriminated between objects in familiar vs. new locations. To eliminate visual/motor deficits or loss of novelty preference as possible explanations for the apparent spatial memory deficits, we also tested whether these mice were impaired in an object-based novelty task involving novel object recognition. When spatial cues are relevant for identifying novel objects, this task requires normal hippocampal function [89,91,92], although hippocampal involvement in this task may be more related to long-term memory, rather than the type of short-term memory that we tested [90,93–97]. Although both the control and experimental groups of mice showed equivalent performance in the test for object novelty, the experimental mice that received the NLGN2 vector were impaired in their performance on tasks involving object-location spatial memory. Furthermore, these mice showed spatial memory deficits when compare to controls in the Morris water maze. On the first two days of training, when the escape platform location was visible using a local cue, both groups performed equivalently, demonstrating equivalent abilities to locate and escape out of the water onto the platform. However, removal of the local cue on the platform on day 3, forced the mice to navigate using memory and distal visual cues. With this more difficult spatial navigation task, the mice that received the AAV-NLGN2 vector were significantly worse than controls, suggesting that overexpression of NGLN2 interferes with spatial memory acquisition (Figure 8 F). Interestingly, these deficits in the probe trial were modest; while the mice with AAV-NLGN2 crossed the platform area significantly fewer times and showed a trend towards higher latencies to first platform crossing, they did not exhibit significant deficits in the time spent in the correct quadrant. Thus, overexpression of AAV-NLGN2 may impair the acquisition of object-based spatial memories, rather than the recall of those memories. One possible explanation for our findings is that increased expression of NLGN2 may alter the receptive field properties of hippocampal place cells, which form a finely-tuned “mental map” composed of discrete receptive fields that activate and deactivate as an animal moves through space [98–104]. Given the evidence that GABAergic neurons in the hippocampus and entorhinal cortex play key roles in defining hippocampal place cell receptive field properties [105–107] and regulating theta rhythms [37,107,108], future experiments could investigate whether NLGN2 overexpression in the hippocampus selectively disrupts the receptive field properties or firing rates of place cells during spatial memory acquisition tasks, while leaving other types of object recognition memory intact [109–114].

5. Conclusions

This study showed that NLGN2 overexpression may induce *de novo* synaptic changes in the adult mouse hippocampus, which functionally impact hippocampal-dependent behaviors. Our studies showed that hippocampal transduction of AAV-NLGN2 increased localization of inhibitory synaptic proteins to putative pre and postsynaptic sites. These findings correlated with deficits in hippocampal-dependent behavior and memory formation.

Funding

This work was supported by grants from Citizens United for Research in Epilepsy(JRN), NINDS 1R15NS072879 (JRN), the CT Regenerative Medicine Fund (JRN), and pilot grant funding from Wesleyan University.

Acknowledgements

We would like to thank Jyoti Gupta, Muhammad Nauman Arshad, and Swechhya Shrestha for their insightful comments on this project and technical help. We also wish to thank Dan Lawrence, Luis Gonzalez, Kevin Cobbol, and Jaye Jeong for help with data analyses, and Wesleyan University Quantitative Analysis Center for assistance with statistical analyses.

Appendix A. Supplementary data

Supplementary data associated with this article can be found, in the online version, at https://doi.org/10.1016/j.bbr.2018.12.052.

References

[1] F. Varoqueaux, S. Jamain, N. Brose, Neuroligin 2 is exclusively localized to inhibitory synapses, Eur. J. Cell Biol. 83 (9) (2004) 449–456.
[2] A.A. Chubykin, D. Atasoy, M.R. Etherton, N. Brose, E.T. Kavalali, J.R. Gibson, T.C. Südhof, Activity-dependent validation of excitatory versus inhibitory synapses by neuroligin-1 versus neuroligin-2, Neuron 54 (6) (2007) 919–931.
[3] A. Poulopoulos, G. Aramuni, G. Meyer, T. Soykan, M. Hoon, T. Papadopoulos, M. Zhang, I. Paarmann, C. Fuchs, K. Harvey, P. Jedlicka, S.W. Schwarzacher, H. Betz, R.J. Harvey, N. Brose, W. Zhang, F. Varoqueaux, Neuroligin 2 drives postsynaptic assembly at perisomatic inhibitory synapses through gephyrin and collybistin, Neuron 63 (5) (2009) 628–642.
[4] J.N. Levinson, R. Li, R. Kang, H. Moukhles, A. El-Husseini, S.X. Bamji, Postsynaptic scaffolding molecules modulate the localization of neuroligins, Neuroscience 165 (3) (2010) 782–793.
[5] T.J. Siddiqui, A.M. Craig, Synaptic organizing complexes, Curr. Opin. Neurobiol. 21 (1) (2011) 132–143.
[6] T. Nguyen, T.C. Südhof, Binding properties of neuroligin 1 and neurexin 1 reveal function as heterophilic cell adhesion molecules, J. Biol. Chem. 272 (41) (1997) 26032–26039.
[7] M.F. Lisé, A. El-Husseini, The neuroligin and neurexin families: from structure to

function at the synapse, Cell. Mol. Life Sci. 63 (16) (2006) 1833–1849.
[8] K. Futai, C.D. Doty, B. Baek, J. Ryu, M. Sheng, Specific trans-synaptic interaction with inhibitory interneuronal neurexin underlies differential ability of neuroligins to induce functional inhibitory synapses, J. Neurosci. 33 (8) (2013) 3612–3623.
[9] D.J. Parente, C. Garriga, B. Baskin, G. Douglas, M.T. Cho, G.C. Araujo, M. Shinawi, Neuroligin 2 nonsense variant associated with anxiety, autism, intellectual disability, hyperphagia, and obesity, Am. J. Med. Genet. Part A 173 (1) (2017) 213–216.
[10] S. Jamain, H. Quach, C. Betancur, M. Råstam, C. Colineaux, C.I. Gillberg, H. Soderstrom, B. Giros, M. Leboyer, C. Gillberg, T. Bourgeron, C. Gillberg, A. Nydén, H. Söderström, A. Philippe, D. Cohen, N. Chabane, M.-C. Mouren-Siméoni, A. Brice, E. Sponheim, I. Spurkland, O.H. Skjeldal, M. Coleman, P.L. Pearl, I.L. Cohen, J. Tsiouris, M. Zappella, G. Menchetti, A. Pompella, H. Aschauer, L. Maldergem, Mutations of the X-linked genes encoding neuroligins NLGN3 and NLGN4 are associated with autism, Nat. Genet. 34 (1) (2003) 27–29.
[11] K.L. Pettem, D. Yokomaku, H. Takahashi, Y. Ge, A. Craig, Interaction between autism-linked MDGAs and neuroligins suppresses inhibitory synapse development, J. Cell Biol. 200 (3) (2013) 321–336.
[12] C. Sun, M.-C. Cheng, R. Qin, D.-L. Liao, T.-T. Chen, F.-J. Koong, G. Chen, C.-H. Chen, Identification and functional characterization of rare mutations of the neuroligin-2 gene (NLGN2) associated with schizophrenia, Hum. Mol. Genet. 20 (15) (2011) 3042–3051.
[13] M. Maćkowiak, P. Mordalska, K. Wędzony, Neuroligins, synapse balance and neuropsychiatric disorders, Pharmacol. Rep. 66 (5) (2014) 830–835.
[14] T.C. Südhof, Neuroligins and neurexins link synaptic function to cognitive disease, Nature 455 (7215) (2008) 903–911.
[15] P. Scheiffele, J. Fan, J. Choih, R. Fetter, T. Serafini, Neuroligin expressed in nonneuronal cells triggers presynaptic development in contacting axons, Cell 101 (6) (2000) 657–669.
[16] E.R. Graf, X. Zhang, S.-X.X. Jin, M.W. Linhoff, A.M. Craig, Neurexins induce differentiation of GABA and glutamate postsynaptic specializations via neuroligins, Cell 119 (7) (2004) 1013–1026.
[17] N. Dong, J. Qi, G. Chen, Molecular reconstitution of functional GABAergic synapses with expression of neuroligin-2 and GABAA receptors, Mol. Cell. Neurosci. 35 (1) (2007) 14–23.
[18] J. Li, W. Han, K.A. Pelkey, J. Duan, X. Mao, Y.-X.X. Wang, M.T. Craig, L. Dong, R.S. Petralia, C.J. McBain, W. Lu, Molecular dissection of neuroligin 2 and Slitrk3 reveals an essential framework for GABAergic synapse development, Neuron 96 (4) (2017) 808–995621376.
[19] F. Varoqueaux, G. Aramuni, R.L. Rawson, R. Mohrmann, M. Missler, K. Gottmann, W. Zhang, T.C. Südhof, N. Brose, Neuroligins determine synapse maturation and function, Neuron 51 (6) (2006) 741–754.
[20] Z. Fu, S. Vicini, Neuroligin-2 accelerates GABAergic synapse maturation in cerebellar granule cells, Mol. Cell. Neurosci. 42 (1) (2009) 45–55.
[21] R.M. Hines, L. Wu, D.J. Hines, H. Steenland, S. Mansour, R. Dahlhaus, R.R. Singaraja, X. Cao, E. Sammler, S.G. Hormuzdi, M. Zhuo, A. El-Husseini, Synaptic imbalance, stereotypies, and impaired social interactions in mice with altered neuroligin 2 expression, J. Neurosci. 28 (24) (2008) 6055–6067.
[22] J. Dachtler, J. Glasper, R.N. Cohen, J.L. Ivorra, D.J. Swiffen, A.J. Jackson, M.K. Harte, R.J. Rodgers, S.J. Clapcote, Deletion of α-neurexin II results in autism-related behaviors in mice, Transl. Psychiatry 4 (2014).
[23] J. Blundell, K. Tabuchi, M.F. Bolliger, C.A. Blaiss, N. Brose, X. Liu, T.C. Südhof, C.M. Powell, Increased anxiety-like behavior in mice lacking the inhibitory synapse cell adhesion molecule neuroligin 2, Genes Brain Behav. 8 (1) (2009) 114–126.
[24] O. Babaev, P. Botta, E. Meyer, C. Müller, H. Ehrenreich, N. Brose, A. Lüthi, D. Krueger-Burg, Neuroligin 2 deletion alters inhibitory synapse function and anxiety-associated neuronal activation in the amygdala, Neuropharmacology 100 (2016) 56–65.
[25] C. Kohl, O. Riccio, J. Grosse, O. Zanoletti, C. Fournier, M.V. Schmidt, C. Sandi, Hippocampal neuroligin-2 overexpression leads to reduced aggression and inhibited novelty reactivity in rats, PLoS One 8 (2) (2013).
[26] R.M. Hines, L. Wu, D.J. Hines, H. Steenland, S. Mansour, R. Dahlhaus, R.R. Singaraja, X. Cao, E. Sammler, S.G. Hormuzdi, M. Zhuo, A. El-Husseini, Synaptic imbalance, stereotypies, and impaired social interactions in mice with altered neuroligin 2 expression, J. Neurosci. 28 (24) (2008) 6055–6067.
[27] C. Kohl, X.-D.D. Wang, J. Grosse, C. Fournier, D. Harbich, S. Westerholz, J.-T.T. Li, A. Bacq, C. Sippel, F. Hausch, C. Sandi, M.V. Schmidt, Hippocampal neuroligin-2 links early-life stress with impaired social recognition and increased aggression in adult mice, Psychoneuroendocrinology 55 (2015) 128–143.
[28] L. Danglot, A. Triller, S. Marty, The development of hippocampal interneurons in rodents, Hippocampus 16 (12) (2006) 1032–1060.
[29] F.L. Hitti, S.A. Siegelbaum, The hippocampal CA2 region is essential for social memory, Nature 508 (7494) (2014) 88–92.
[30] F. Leroy, D.H. Brann, T. Meira, S.A. Siegelbaum, Input-timing-dependent plasticity in the hippocampal CA2 region and its potential role in social memory, Neuron 95 (5) (2017) 1089–110200000.
[31] Y. Andrews-Zwilling, A.K. Gillespie, A.V. Kravitz, A.B. Nelson, N. Devidze, I. Lo, S. Yoon, N. Bien-Ly, K. Ring, D. Zwilling, G.B. Potter, J.L.R. Rubenstein, A.C. Kreitzer, Y. Huang, Hilar GABAergic interneuron activity controls spatial learning and memory retrieval, PLoS One 7 (7) (2012).
[32] O. Paulsen, E. Moser, A model of hippocampal memory encoding and retrieval: GABAergic control of synaptic plasticity, Trends Neurosci. 21 (7) (1998) 273–278.
[33] Z. Borhegyi, V. Varga, N. Szilágyi, D. Fabo, T.F. Freund, Phase segregation of medial septal GABAergic neurons during hippocampal theta activity, J. Neurosci. 24 (39) (2004) 8470–8479.
[34] L. Chauvière, N. Rafrafi, C. Thinus-Blanc, F. Bartolomei, M. Esclapez, C. Bernard, Early deficits in spatial memory and theta rhythm in experimental temporal lobe epilepsy, J. Neurosci. 29 (17) (2009) 5402–5410.
[35] V. Cutsuridis, M. Hasselmo, GABAergic contributions to gating, timing, and phase precession of hippocampal neuronal activity during theta oscillations, Hippocampus 22 (7) (2012) 1597–1621.
[36] J. Gan, S.-m. Weng, A.J. Pernía-Andrade, J. Csicsvari, P. Jonas, Phase-locked inhibition, but not excitation, underlies hippocampal ripple oscillations in awake mice in vivo, Neuron 93 (2) (2017) 308–314.
[37] G.R. Richard, A. Titiz, A. Tyler, G.L. Holmes, R.C. Scott, P.P. Lenck-Santini, Speed modulation of hippocampal theta frequency correlates with spatial memory performance, Hippocampus 23 (12) (2013) 1269–1279.
[38] B. Amilhon, C. Huh, F. Manseau, G. Ducharme, H. Nichol, A. Adamantidis, S. Williams, Parvalbumin interneurons of hippocampus tune population activity at theta frequency, Neuron 86 (5) (2015) 1277–1289.
[39] S. Zhao, J.T. Ting, H.E. Atallah, L. Qiu, J. Tan, B. Gloss, G.J. Augustine, K. Deisseroth, M. Luo, A.M. Graybiel, G. Feng, Cell type–specific channelrhodopsin-2 transgenic mice for optogenetic dissection of neural circuitry function, Nat. Methods 8 (9) (2011) 745–752.
[40] Y. Huang, S. Yang, Z.-Y. Hu, G. Lin, W.-X. Zhou, Y.-X. Zhang, A new approach to location of the dentate gyrus and perforant path in rats/mice by landmarks on the skull, Acta Neurobiol. Exp. 72 (2012).
[41] L.B. Tucker, J.T. McCabe, Behavior of male and female C57BL/6J mice is more consistent with repeated trials in the elevated zero maze than in the elevated plus maze, Front. Behav. Neurosci. 11 (2017) 13.
[42] J.L. Silverman, M. Yang, C. Lord, J.N. Crawley, Behavioural phenotyping assays for mouse models of autism, Nat. Rev. Neurosci. 11 (7) (2010) 490.
[43] O. Kaidanovich-Beilin, T. Lipina, I. Vukobradovic, J. Roder, J.R. Woodgett, Assessment of social interaction behaviors, J. Vis. Exp.: JoVE 48 (2011) 2473.
[44] S.S. Moy, J.J. Nadler, A. Perez, R.P. Barbaro, J.M. Johns, T.R. Magnuson, J. Piven, J.N. Crawley, Sociability and preference for social novelty in five inbred strains: an approach to assess autistic-like behavior in mice, Genes Brain Behav. 3 (5) (2004) 287–302.
[45] G. Lindzey, H. Winston, M. Manosevitz, Social dominance in inbred mouse strains, Nature 191 (4787) (1961) 474–476.
[46] D.M. Ippolito, C. Eroglu, Quantifying synapses: an immunocytochemistry-based assay to quantify synapse number, J. Vis. Exp. 45 (2010).
[47] M.E. Horn, R.A. Nicoll, Somatostatin and parvalbumin inhibitory synapses onto hippocampal pyramidal neurons are regulated by distinct mechanisms, Proc. Natl. Acad. Sci. U. S. A. 115 (3) (2018) 589–594.
[48] S. Gangwar, X. Zhong, S. Seshadrinathan, H. Chen, M. Machius, G. Rudenko, Molecular mechanism of MDGA1: regulation of neuroligin 2: neurexin trans-synaptic bridges, Neuron 94 (6) (2017) 1132–11410000.
[49] X. Hu, J.-h. Luo, J. Xu, The interplay between synaptic activity and neuroligin function in the CNS, Biomed Res. Int. 2015 (2015) 498957.
[50] C. Essrich, M. Lorez, J.A. Benson, J.M. Fritschy, B. Lüscher, Postsynaptic clustering of major GABAA receptor subtypes requires the gamma 2 subunit and gephyrin, Nat. Neurosci. 1 (7) (1998) 563–571.
[51] X. Wu, Z. Wu, G. Ning, Y. Guo, R. Ali, R.L. Macdonald, A.L. Blas, B. Luscher, G. Chen, γ-Aminobutyric acid type a (GABAA) receptor α subunits play a direct role in synaptic versus extrasynaptic targeting, J. Biol. Chem. 287 (33) (2012) 27417–27430.
[52] M. Hoon, T. Soykan, B. Falkenburger, M. Hammer, A. Patrizi, K.-F.F. Schmidt, M. Sassoè-Pognetto, S. Löwel, T. Moser, H. Taschenberger, N. Brose, F. Varoqueaux, Neuroligin-4 is localized to glycinergic postsynapses and regulates inhibition in the retina, Proc. Natl. Acad. Sci. U. S. A. 108 (7) (2011) 3053–3058.
[53] J.S. Polepalli, H. Wu, D. Goswami, C.H. Halpern, T.C. Südhof, R.C. Malenka, Modulation of excitation on parvalbumin interneurons by neuroligin-3 regulates the hippocampal network, Nat. Neurosci. 20 (2) (2017) 219–229.
[54] M.A. Bemben, S.L. Shipman, R.A. Nicoll, K.W. Roche, The cellular and molecular landscape of neuroligins, Trends Neurosci. 38 (8) (2015) 496–505.
[55] S. Chanda, W.D. Hale, B. Zhang, M. Wernig, T.C. Südhof, Unique vs. redundant functions of neuroligin genes in shaping excitatory and inhibitory synapse properties, J. Neurosci. (2017) 125-117.
[56] C. Miao, Q. Cao, M.-B. Moser, E.I. Moser, Parvalbumin and somatostatin interneurons control different space-coding networks in the medial entorhinal cortex, Cell 171 (3) (2017) 507-1574567936.
[57] A.J. Murray, J.-F. Sauer, G. Riedel, C. McClure, L. Ansel, L. Cheyne, M. Bartos, W. Wisden, P. Wulff, Parvalbumin-positive CA1 interneurons are required for spatial working but not for reference memory, Nat. Neurosci. 14 (3) (2011).
[58] C. Fuchs, K. Abitbol, J.J. Burden, A. Mercer, L. Brown, J. Iball, A.F. Stephenson, A.M. Thomson, J.N. Jovanovic, GABAA receptors can initiate the formation of functional inhibitory GABAergic synapses, Eur. J. Neurosci. 38 (8) (2013) 3146–3158.
[59] P. Panzanelli, S. Früh, J.-M. Fritschy, Differential role of GABAA receptors and neuroligin 2 for perisomatic GABAergic synapse formation in the hippocampus, Brain Struct. Funct. (2017) 1–13.
[60] A. Patrizi, B. Scelfo, L. Viltono, F. Briatore, M. Fukaya, M. Watanabe, P. Strata, F. Varoqueaux, N. Brose, J.-M. Fritschy, M. Sassoè-Pognetto, Synapse formation and clustering of neuroligin-2 in the absence of GABAA receptors, Proc. Natl. Acad. Sci. U. S. A. 105 (35) (2008) 13151–13156.
[61] C. Betancur, T. Sakurai, J.D. Buxbaum, The emerging role of synaptic cell-adhesion pathways in the pathogenesis of autism spectrum disorders, Trends Neurosci. 32 (7) (2009) 402–412.
[62] J. Gauthier, T.J. Siddiqui, P. Huashan, D. Yokomaku, F.F. Hamdan, N. Champagne, M. Lapointe, D. Spiegelman, A. Noreau, R.G. Lafrenière, F. Fathalli, R. Joober, M.-

O. Krebs, L.E. DeLisi, L. Mottron, É. Fombonne, J.L. Michaud, P. Drapeau, S. Carbonetto, A. Craig, G.A. Rouleau, Truncating mutations in NRXN2 and NRXN1 in autism spectrum disorders and schizophrenia, Hum. Genet. 130 (4) (2011) 563–573.
[63] J. Li, A. Yoshikawa, M.D. Brennan, T.L. Ramsey, H.Y. Meltzer, Genetic predictors of antipsychotic response to lurasidone identified in a genome wide association study and by schizophrenia risk genes, Schizophr. Res. 192 (2018).
[64] A. Lawson-Yuen, J.-S. Saldivar, S. Sommer, J. Picker, Familial deletion within NLGN4 associated with autism and Tourette syndrome, Eur. J. Hum. Genet. 16 (5) (2008) 5202006.
[65] H. Jin, H. Wu, G. Osterhaus, J. Wei, K. Davis, D. Sha, E. Floor, C.-C. Hsu, R.D. Kopke, J.-Y. Wu, Demonstration of functional coupling between γ-aminobutyric acid (GABA) synthesis and vesicular GABA transport into synaptic vesicles, Proc. Natl. Acad. Sci. U. S. A. 100 (7) (2003) 4293–4298.
[66] T.C. Jacob, Y.D. Bogdanov, C. Magnus, R.S. Saliba, J.T. Kittler, P.G. Haydon, S.J. Moss, Gephyrin regulates the cell surface dynamics of synaptic GABAA receptors, J. Neurosci. 25 (45) (2005) 10469–10478.
[67] M. Kneussel, J.H. Brandstätter, B. Laube, S. Stahl, U. Müller, H. Betz, Loss of postsynaptic GABA(A) receptor clustering in gephyrin-deficient mice, J. Neurosci. 19 (21) (1999) 9289–9297.
[68] C. Essrich, M. Lorez, J.A. Benson, J.-M. Fritschy, B. Lüscher, Postsynaptic clustering of major GABAA receptor subtypes requires the γ2 subunit and gephyrin, Nat. Neurosci. 1 (7) (1998) 563–571.
[69] L. Saiepour, C. Fuchs, A. Patrizi, M. Sassoè-Pognetto, R.J. Harvey, K. Harvey, Complex role of collybistin and gephyrin in GABAA receptor clustering, J. Biol. Chem. 285 (38) (2010) 29623–29631.
[70] P. Jedlicka, M. Hoon, T. Papadopoulos, A. Vlachos, R. Winkels, A. Poulopoulos, H. Betz, T. Deller, N. Brose, F. Varoqueaux, S.W. Schwarzacher, Increased dentate gyrus excitability in neuroligin-2-deficient mice in vivo, Cereb. Cortex 21 (2) (2011) 357–367.
[71] J. Artinian, J.-C. Lacaille, Disinhibition in learning and memory circuits: new vistas for somatostatin interneurons and long-term synaptic plasticity, Brain Res. Bull. 141 (2017) 20–26.
[72] L. Acsady, T.J. Görcs, T.F. Freund, Different populations of vasoactive intestinal polypeptide-immunoreactive interneurons are specialized to control pyramidal cells or interneurons in the hippocampus, Neuroscience 73 (2) (1996) 317–334.
[73] J. Basu, J.D. Zaremba, S.K. Cheung, F.L. Hitti, B.V. Zemelman, A. Losonczy, S.A. Siegelbaum, Gating of hippocampal activity, plasticity, and memory by entorhinal cortex long-range inhibition, Science 351 (6269) (2016) aaa5694.
[74] H. Bao, B. Asrican, W. Li, B. Gu, Z. Wen, S.-A. Lim, I. Haniff, C. Ramakrishnan, K. Deisseroth, B. Philpot, J. Song, Long-range GABAergic inputs regulate neural stem cell quiescence and control adult hippocampal neurogenesis, Cell Stem Cell 21 (5) (2017) 604–61700000.
[75] S. Jamain, K. Radyushkin, K. Hammerschmidt, S. Granon, S. Boretius, F. Varoqueaux, N. Ramanantsoa, J. Gallego, A. Ronnenberg, D. Winter, J. Frahm, J. Fischer, T. Bourgeron, H. Ehrenreich, N. Brose, Reduced social interaction and ultrasonic communication in a mouse model of monogenic heritable autism, Proc. Natl. Acad. Sci. U. S. A. 105 (5) (2008) 1710–1715.
[76] M.P. Richardson, B.A. Strange, R.J. Dolan, Encoding of emotional memories depends on amygdala and hippocampus and their interactions, Nat. Neurosci. 7 (3) (2004) 278–285.
[77] J.H. Kogan, P.W. Franklandand, A.J. Silva, Long-term memory underlying hippocampus-dependent social recognition in mice, Hippocampus 10 (1) (2000) 47–56.
[78] E.L. Stevenson, H.K. Caldwell, Lesions to the CA2 region of the hippocampus impair social memory in mice, Eur. J. Neurosci. 40 (9) (2014) 3294–3301.
[79] T. Tanimizu, J.W. Kenney, E. Okano, K. Kadoma, P.W. Frankland, S. Kida, Functional connectivity of multiple brain regions required for the consolidation of social recognition memory, J. Neurosci. 37 (15) (2017) 4103–4116.
[80] A. Mercer, H.L. Trigg, A.M. Thomson, Characterization of neurons in the CA2 subfield of the adult rat Hippocampus, J. Neurosci. 27 (27) (2007) 7329–7338.
[81] T. Raam, K.M. McAvoy, A. Besnard, A.H. Veenema, A. Sahay, Hippocampal oxytocin receptors are necessary for discrimination of social stimuli, Nat. Commun. 8 (1) (2017) 2001.
[82] T. Okuyama, T. Kitamura, D.S. Roy, S. Itohara, S. Tonegawa, Ventral CA1 neurons store social memory, Science 353 (6307) (2016) 1536–1541.
[83] M.-C. Chiang, A. Huang, M.E. Wintzer, T. Ohshima, T.J. McHugh, A role for CA3 in social recognition memory, Behav. Brain Res. 354 (2018) 22–30.
[84] M.A. van der Kooij, M. Fantin, I. Kraev, I. Korshunova, J. Grosse, O. Zanoletti, R. Guirado, C. Garcia-Mompó, J. Nacher, M.G. Stewart, V. Berezin, C. Sandi, Impaired hippocampal neuroligin-2 function by chronic stress or synthetic peptide treatment is linked to social deficits and increased aggression, Neuropsychopharmacology 39 (5) (2014) 1148.
[85] A. Katzman, C.M. Alberini, NLGN1 and NLGN2 in the prefrontal cortex: their role in memory consolidation and strengthening, Curr. Opin. Neurobiol. 48 (2018) 122–130.
[86] J. Liang, W. Xu, Y.T. Hsu, A.X. Yee, L. Chen, T.C. Südhof, Conditional neuroligin-2 knockout in adult medial prefrontal cortex links chronic changes in synaptic inhibition to cognitive impairments, Mol. Psychiatry 20 (7) (2015) 850–859.
[87] C.-H. Chen, P.-W. Lee, H.-M. Liao, P.-K. Chang, Neuroligin 2 R215H mutant mice manifest anxiety, increased prepulse inhibition, and impaired spatial learning and memory, Front. Psychiatry 8 (2017) 257.
[88] A. Ennaceur, N. Neave, J.P. Aggleton, Spontaneous object recognition and object location memory in rats: the effects of lesions in the cingulate cortices, the medial prefrontal cortex, the cingulum bundle and the fornix, Exp. Brain Res. 113 (3) (1997) 509–519.
[89] M. Antunes, G. Biala, The novel object recognition memory: neurobiology, test procedure, and its modifications, Cogn. Process. 13 (2) (2012) 93–110.
[90] E. Dere, J.P. Huston, M.A. De Souza Silva, The pharmacology, neuroanatomy and neurogenetics of one-trial object recognition in rodents, Neurosci. Biobehav. Rev. 31 (5) (2007) 673–704.
[91] N.J. Broadbent, S. Gaskin, L.R. Squire, R.E. Clark, Object recognition memory and the rodent hippocampus, Learn. Mem. 17 (1) (2010) 5–11.
[92] S.J. Cohen, R.W. Stackman Jr, Assessing rodent hippocampal involvement in the novel object recognition task. A review, Behav. Brain Res. 285 (2015) 105–117.
[93] A. Oliveira, J.D. Hawk, T. Abel, R. Havekes, Post-training reversible inactivation of the hippocampus enhances novel object recognition memory, Learn. Mem. 17 (3) (2010) 155–160.
[94] G.R.I. Barker, E.C. Warburton, When is the hippocampus involved in recognition memory? J. Neurosci. 31 (29) (2011) 10721–10731.
[95] D.G. Mumby, Perspectives on object-recognition memory following hippocampal damage: lessons from studies in rats, Behav. Brain Res. 127 (1–2) (2001) 159–181.
[96] B.D. Winters, T.J. Bussey, Transient inactivation of perirhinal cortex disrupts encoding, retrieval, and consolidation of object recognition memory, J. Neurosci. 25 (1) (2005) 52–61.
[97] A. Sawangjit, C.N. Oyanedel, N. Niethard, C. Salazar, J. Born, M. Inostroza, The hippocampus is crucial for forming non-hippocampal long-term memory during sleep, Nature 564 (2018) 109–113.
[98] T. Hafting, M. Fyhn, S. Molden, M.-B.B. Moser, E.I. Moser, Microstructure of a spatial map in the entorhinal cortex, Nature 436 (7052) (2005) 801–806.
[99] J. O'Keefe, J. Dostrovsky, The hippocampus as a spatial map. Preliminary evidence from unit activity in the freely-moving rat, Brain Res. 34 (1) (1971) 171–175.
[100] E.T. Rolls, Spatial view cells and the representation of place in the primate hippocampus, Hippocampus 9 (4) (1999) 467–480.
[101] L. Nadel, The hippocampus and space revisited, Hippocampus 1 (3) (1991) 221–229.
[102] A.D. Ekstrom, M.J. Kahana, J.B. Caplan, T.A. Fields, E.A. Isham, E.L. Newman, I. Fried, Cellular networks underlying human spatial navigation, Nature 425 (6954) (2003) 184–188.
[103] N. Ulanovsky, C.F. Moss, Hippocampal cellular and network activity in freely moving echolocating bats, Nat. Neurosci. 10 (2) (2007) 224–233.
[104] S.-J.J. Zhang, J. Ye, J.J. Couey, M. Witter, E.I. Moser, M.-B.B. Moser, Functional connectivity of the entorhinal-hippocampal space circuit, Philos. Trans. R. Soc. Lond. Ser. B: Biol. Sci. 369 (1635) (2014) 20120516.
[105] W.B. Wilent, D.A. Nitz, Discrete place fields of hippocampal formation interneurons, J. Neurophysiol. 97 (6) (2007) 4152–4161.
[106] V. Ego-Stengel, M.A. Wilson, Spatial selectivity and theta phase precession in CA1 interneurons, Hippocampus 17 (2) (2007) 161–174.
[107] B. Hangya, Y. Li, R.U. Muller, A. Czurkó, Complementary spatial firing in place cell-interneuron pairs, J. Physiol. 588 (Pt 21) (2010) 4165–4175.
[108] B. Hangya, Z. Borhegyi, N. Szilágyi, T.F. Freund, V. Varga, B. Hangya, Z. Borhegyi, N. Szilágyi, T.F. Freund, V. Varga, GABAergic neurons of the medial septum lead the hippocampal network during theta activity, J. Neurosci. 29 (25) (2009) 8094–8102.
[109] S.S. Deshmukh, J.J. Knierim, Representation of non-spatial and spatial information in the lateral entorhinal cortex, Front. Behav. Neurosci. 5 (2011) 69.
[110] M. Fyhn, S. Molden, S. Hollup, M.-B.B. Moser, E. Moser, Hippocampal neurons responding to first-time dislocation of a target object, Neuron 35 (3) (2002) 555–566.
[111] K.J. Jeffery, A. Gilbert, S. Burton, A. Strudwick, Preserved performance in a hippocampal dependent spatial task despite complete place cell remapping, Hippocampus 13 (2) (2003) 175–189.
[112] J.J. Knierim, J.P. Neunuebel, S.S. Deshmukh, Functional correlates of the lateral and medial entorhinal cortex: objects, path integration and local–global reference frames, Philos. Trans. R. Soc. Lond. B: Biol. Sci. 369 (1635) (2014) 20130369.
[113] M.W. Jones, M.A. Wilson, Theta rhythms coordinate hippocampal-prefrontal interactions in a spatial memory task, PLoS Biol. 3 (12) (2005).
[114] D. Wilson, R.F. Langston, M.I. Schlesiger, M. Wagner, S. Watanabe, J.A. Ainge, Lateral entorhinal cortex is critical for novel object-context recognition, Hippocampus 23 (5) (2013) 352–366.